Predicting and mitigating the net greenhouse gas emissions of crop rotations in Western Europe

Simon Lehuger, Benoit Gabrielle, Patricia Laville, Matieyendou Lamboni, Benjamin Loubet, Pierre Cellier

Predicting and mitigating the net greenhouse gas emissions of crop rotations in Western Europe

Simon Lehuger[a,b 1] , Benoît Gabrielle[c], Patricia Laville[d], Matieyendou Lamboni[e], Benjamin Loubet[d], Pierre Cellier[d]

a: Agroscope Reckenholz-Tänikon Research Station ART, Air pollution/Climate Group, Reckenholzstrasse 191, 8046 Zurich, Switzerland
b: Now at Cemagref, Environmental Management and Biological Treatment of Wastes Research Unit, 17 Avenue de Cucillé, 35044 Rennes, France.
c: AgroParisTech, UMR 1091 INRA-AgroParisTech Environnement et Grandes Cultures,78850 Thiverval-Grignon, France
d: Institut National de la Recherche Agronomique, UMR 1091 INRA-AgroParisTech Environnement et Grandes Cultures,78850 Thiverval-Grignon, France
e: Institut National de la Recherche Agronomique, UR 341 INRA Mathématiques et Informatique Appliquées, 78352 Jouy-en-Josas, France

[1]Corresponding author: Cemagref, Environmental Management and Biological Treatment of Wastes Research Unit, 17 Avenue de Cucillé, 35044 Rennes, France. E-mail: Simon.Lehuger@cemagref.fr. Fax: +33 (0) 2 23 48 21 15. Phone: +33 (0) 2 99 29 91 56.

Abstract

Nitrous oxide, carbon dioxide and methane are the main biogenic greenhouse gases (GHG) contributing to net greenhouse gas balance of agro-ecosystems. Evaluating the impact of agriculture on climate thus requires capacity to predict the net exchanges of these gases in a systemic approach, as related to environmental conditions and crop management. Here, we used experimental data sets from intensively-monitored cropping systems in France and Germany to calibrate and evaluate the ability of the biophysical crop model CERES-EGC to simulate GHG exchanges at the plot-scale. The experiments involved major crop types (maize-wheat-barley-rapeseed) on loam and rendzina soils. The model was subsequently extrapolated to predict CO_2 and N_2O fluxes over entire crop rotations. Indirect emissions (IE) arising from the production of agricultural inputs and from use of farm machinery were also added to the final greenhouse gas balance. One experimental site (involving a maize-wheat-barley-mustard rotation on a loamy soil) was a net source of GHG with a net GHG balance of 670 kg CO_2-C eq ha^{-1} yr^{-1}, of which half were due to IE and half to direct N_2O emissions. The other site (involving a rapeseed-wheat-barley rotation on a rendzina) was a net sink of GHG for -650 kg CO_2-C eq ha^{-1} yr^{-1}, mainly due to high C returns to soil from crop residues. A selection of mitigation options were tested at one experimental site, of which straw return to soils emerged as the most efficient to reduce the net GHG balance of the crop rotation, with a 35% abatement. Halving the rate of N inputs only allowed a 27% reduction in net GHG balance. Removing the organic fertilizer application led to a substantial loss of C for the entire crop rotation that was not compensated by a significant decrease of N_2O emissions due to a lower N supply in the system. Agro-ecosystem modeling and scenario analysis may therefore contribute to design productive cropping systems with low GHG emissions.

Keywords

Net greenhouse gas balance; Agro-ecosystem model; CERES-EGC; Bayesian calibration; Greenhouse gases; Nitrous oxide; Mitigation

1 Introduction

While the security of food supply to an increasing population has turned into a pressing issue worldwide, the growing environmental footprint of agriculture due to land use change and management intensification is posing a forthcoming challenge (Tilman, 1999). Assessing the contribution of agriculture to climate change is one of the key questions that environmental scientists have to address in order to identify possible measures to reduce the burden of agriculture on global warming (Galloway et al., 2008; Sutton et al., 2007). Agriculture bears a significant contribution to the anthropogenic emissions of greenhouse gases (GHG), with a share estimated at 10-12% of worldwide emissions, corresponding to a net flux of 6.1 Gt CO_2-eq y^{-1} (Smith et al., 2007). In the case of arable crops, the latter figure includes the direct exchanges of GHGs between agro-ecosystems and the atmosphere, but not the upstream (indirect) emissions resulting from the use of agricultural inputs and farm machinery, which should also be attributed to agricultural activities (Ceschia et al., 2010). Direct emissions of GHG are made up of three terms: emissions of nitrous oxide, net carbon fluxes between soil-plant systems and the atmosphere, and methane exchanges. Nitrous oxide (N_2O) is produced by soil micro-organisms via the processes of nitrification and denitrification (Hutchinson and Davidson, 1993). Arable soils are responsible for 60% of the global anthropogenic emissions of N_2O (Smith et al., 2007), and their source strength primarily depends on the fertilizer N inputs necessary for crop production. Other environmental factors regulate these emissions including soil temperature, soil moisture, soil NO_3^- and NH_4^+ concentrations, and the availability of organic C substrate to micro-organisms (Conrad, 1996). The effect of these factors results in a large spatial and temporal variability of N_2O emissions (Jungkunst et al., 2006; Kaiser and Ruser, 2000). The second term in the GHG balance, the net C exchange, equals the change in ecosystem C storage. These variations reflect the balance between C inputs to the agro-ecosystems, via crop residue return, root deposition

and organic amendments, and outputs via harvested biomass, soil organic matter mineralization, erosion and leaching. At the rotation scale, the C budget is the balance between the net ecosystem production plus the import of organic C from manure application minus the C in harvested biomass (Ammann et al., 2007; Ceschia et al., 2010; Grant et al., 2007). Lastly, non-flooded cropland is usually considered a weak methane-sink that mitigates the GHG balance of cropping systems by 1% to 3% (Mosier et al., 2005; Robertson et al., 2000).

Indirect emissions of GHG arising from the production of agricultural inputs (fertilizers, pesticides and lime), fuel combustion and use of machinery on the farm may contribute as much as half of the total GHG budget of agricultural crops (Adviento-Borbe et al., 2007; Mosier et al., 2005; Robertson et al., 2000). Thus, reducing the indirect emissions provides high potential to mitigate the GHG budget of crop production (West and Marland, 2002).

The global GHG budget of an agro-ecosystem may be expressed in CO_2 equivalents, using the GWPs of all the trace gases with radiative forcing (IPCC, 2007). Various agricultural practices impact the GHG balance of agro-ecosystems. Some of them may first enhance the carbon sink-strength of soils: conversion to no-tillage practices, the introduction of catch crops, and the incorporation of crop residues into the topsoil were shown to lead to possible C sequestration into the organic carbon pool of agricultural soils (Arrouays et al., 2002; Smith et al., 2001). The evaluation of candidate agricultural practices to reduce the net GHG balance of agro-ecosystems should encompass indirect and direct emissions of all GHG, to avoid trade-off effects. For instance, because the C and N biogeochemical cycles are interconnected, increased CH_4 and N_2O emissions may offset the beneficial C storage associated with minimum tillage practices aiming at sequestering C in soil (Desjardins et al., 2005; Li et al., 2005a; Six et al., 2004).

In a given rotation, the previous crop affect the crop that follows because the crop sequence has an effect on the nutrients' turn-over, and soil organic and mineral status. In addition, the nutrients derived from fertilizers or biological fixation may be recycled or stored into the pools of the

soil organic matter (SOM), and may be re-emitted into air or water in subsequent years (Anthoni et al., 2004; Del Grosso et al., 2005). Calculating the net GHG balance of a complete sequence of crops is more relevant than calculating that of one single crop.

Estimates of net GHG emissions from agro-ecosystems have been used to assess the effect of the conversion to a new management practice, e.g., no-till, catch crops, farmyard manure application, or land use change (Bhatia et al., 2005; Mosier et al., 2005; Robertson et al., 2000), or for inclusion into the life cycle assessment of a crop-derived product. These include biofuels, animal feed, or human food (Adler et al., 2007; Gabrielle and Gagnaire, 2008; Kim and Dale, 2005). Direct GHG emissions may be either estimated from direct field measurements (Adviento-Borbe et al., 2007; Bhatia et al., 2005; Ceschia et al., 2010; Mosier et al., 2005; Robertson et al., 2000), or by using biogeochemical models simulating GHG emissions (Adler et al., 2007; Del Grosso et al., 2005; Desjardins et al., 2005; Pathak et al., 2005). Most agro-ecosystems have a positive net GHG balance (meaning they enhance global warming), but this trend is mainly controlled by the C storage potential of the soil. In the US Midwest, Robertson et al. (2000) measured the net GHG balance of an annual crop rotation (maize-soybean-wheat) as 40 and 310 kg CO_2-C eq ha^{-1} yr^{-1} for no-till and conventional tillage systems, respectively. In Colorado, for rainfed crops under no-till practices, Mosier et al. (2005) measured a topsoil C-storage of about 300 kg CO_2-C eq ha^{-1} yr^{-1} in perennial, rainfed crops under no-till, which offset the other terms in the GHG balance and resulted in a negative net GHG balance of -85 kg CO_2-C eq ha^{-1} yr^{-1}. Adviento-Borbe et al. (2007) quantified GHG balances in four high-yielding maize systems in Nebraska (USA) for continuous system and maize-soybean rotations, with recommended and intensive management for both systems. They reported that the N_2O fluxes were similar across the two treatments despite the large differences in crop management and N fertilizer applications. As a result, all the systems were net sources of GHGs with GHG balances between 540 and 1020 kg CO_2-C eq ha^{-1} yr^{-1}.

Indirect emissions may be easily calculated thanks to databases of life cycle inventories (Nemecek et al., 2003; West and Marland, 2002), but direct field emissions of N_2O and C storage in soil are extremely dependent of pedoclimatic conditions and agricultural management practices. To take into account these sources of variability, and to devise mitigation strategies, the processes occurring in the soil-crop-atmosphere system should be modeled simultaneously, together with the effect of agricultural practices. In the past, modeling approaches were developed in parallel either by agronomists seeking to predict crop growth and yields in relation to their management (Boote et al., 1996), or by ecologists focusing on biogeochemical cycles and in particular mineralization, nitrification and denitrification in soils (e.g., Li et al., 1992). With the increasing interest in the prediction of trace gas emissions from arable soils (or pollutants in general), both approaches have already been linked together in a more systemic perspective (Gijsman et al., 2002; Zhang et al., 2002). The CERES-EGC model was designed following this purpose to estimate site-and-management specific environmental impacts, or regionalised inventories of trace gas emissions (Gabrielle et al., 2006; Rolland et al., 2010).

The objectives of this work were: i/ to test and calibrate the CERES-EGC crop model with experimental data from cropping systems representative of Western Europe, ii/ to apply the model to assess the net GHG balance of the cropping systems, including direct and indirect emissions of GHG and iii/ to assess mitigation options for net GHG emission reduction for a set of agricultural practices in Western Europe.

2 Material and Methods

2.1 Experimental data

2.1.1 Field sites

The field experiments were carried out at three locations in Western Europe, at Rafidin (northern France, 48.5 N, 2.15 E) in the Champagne region in 1994-1995 (Gosse et al., 1999), at Grignon

near the city of Paris (northern France, 48.9 N, 1.95 E) in 2004-2008 (Loubet et al., 2011) and at Gebesee (20 km NW of Erfurt in Germany, 51.1 N, 10.9 E) in 2006-2007 (Skiba et al., 2009).

At Rafidin, the soil was a grey rendzina overlying a subsoil of mixed compact and cryoturbed chalk. The topsoil (0-30 cm) has a clay loam texture with 31% clay and 28% sand, an organic matter content of 19.5 g kg^{-1}, a pH (water) of 8.3, and a bulk density of 1.23 Mg m^{-3}. At Grignon, the soil was a silt loam with 18.9% clay and 71.3% silt in the topsoil. In the top 15 cm, organic carbon content was 20.0 g kg^{-1}, the pH (water) was 7.6 and the bulk density 1.30 Mg m^{-3}. At Gebesee, the soil was a Chernozerm (silty clay loam) with 35.8% clay and 60.3% silt in the top 20 cm, organic carbon was 23.0 g kg^{-1}, the pH (water) was 6.7 and the bulk density 1.3 Mg m^{-3}.

Table 1 recapitulates the crop sequences of the experimental sites and the main cropping operations. The Rafidin site involved a rapeseed - winter wheat - winter barley rotation, and the measurements essentially took place during the rapeseed growing cycle, from its sowing on 9 Sept., 1994 to its harvest on 11 July, 1995. Three fertilizer N treatments (N0=0 kg N ha^{-1}, N1=155 kg N ha^{-1} and N2=242 kg N ha^{-1}) were set up on 30×30 m blocks arranged in a split-plot design with three replicates. For this site, the rotations we simulated were only different regarding the fertilizer N inputs on the rapeseed crop. The other crops in the rotation (wheat and barley) were managed identically in the N0, N1 and N2 rotations.

At the Grignon site, two experiments were monitored in parallel on two fields: a principal field (Grignon-PP, 19 ha), on which a maize - winter wheat - winter barley - mustard rotation was monitored since 2004 and 3 adjacent plots (Grignon-PAN1, -PAN2, -PAN3, 2500 m^{-2} each) on another field on which the same rotation was applied since 2006, with 0, 1 and 2 years time-lag interval in order to have all the crops each year. The adjacent plots were monitored from July 2007 to September 2008. In the rotation, a mustard was planted following the harvest of barley the year before to serve as a catch crop to reduce nitrate leaching. On the Grignon-PP field, dairy

cow slurry was applied between the harvest of barley and the planting of mustard on 31 August 2004 (60 kg total N ha^{-1} and 45 kg N-NH_4^+ ha^{-1}), and before the maize sowing on 16 April 2008 (80 kg total N ha^{-1} and 60 kg N-NH_4^+ ha^{-1}).

At Gebesee, the 6-ha field was cropped from 2003 to 2007 with a rapeseed - winter barley - sugar beet - winter wheat crop sequence. Two applications of organic fertilizers were carried out in 2007, one application of cattle slurry (18 m^3 ha^{-1}) in the wheat crop on 11 Apr. and 35 t ha^{-1} of farmyard manure on 4 Sept. after harvest. For this site, we only assessed the net greenhouse gas emissions of the winter wheat cycle starting on 27 Oct. 2006 and ending on 5 Oct. 2007.

2.1.2 Soil and crop measurements

Soil mineral nitrogen content (NO_3^- and NH_4^+) and moisture content were monitored in the following layers: 0-15 cm, 15-30 cm, 30-60 cm and 60-90 cm at Grignon, 0-30 cm, 30-60 cm, 60-90 cm, and 90-120 cm at Rafidin, and 0-10 cm and 10-20 cm at Gebesee. Soil samples were taken in triplicates with an automatic (Rafidin) or manual (Grignon and Gebesee) auger every 1 to 4 weeks, and analyzed for moisture content and mineral N. The latter involved an extraction of soil samples with 1 M KCl and colorimetric analysis of the supernatant. At the three sites, soil moisture and temperature were also continuously recorded using TDR (Time Domain Reflectrometry, Campbell Scientific, Logan, Utah, USA) and thermocouples at 5, 10, 20 and 30 cm depth at Grignon, at 8, 16 ,32 and 64 cm depth in Gebesee and at 5, 10, 20 and 45 cm depth at Rafidin (N2 treatment). Soil bulk density was measured once at each site, using steel rings, by layer of 15 cm over 0-60 cm at Grignon, by layer of 10 cm over 0-50 cm at Gebesee and by layer of 30 cm over 0-120 cm at Rafidin. For both experiments of Grignon and Rafidin, plants were collected every 2 to 4 weeks as soon as the plants were growing, and separated into leaves, stems, ears or pods, and roots. On the same as plant sampling, leaf area index was measured with an optical leaf area meter or analysis of leaf scans. The plant samples were dried for 48 h at 80° C

and weighted, and analyzed for C, N, P and K content by flash combustion.

2.1.3 Trace gas fluxes and micrometeorological measurements

At the three sites, daily climatic data were recorded with an automatic meteorological station, including maximum and minimum daily air temperatures (° C), rainfall (mm day^{-1}), solar radiation (MJ m^{-2} day^{-1}) and wind speed (m s^{-1}). The monitoring periods of GHGs for the 3 sites are summarized in Table 1. At Grignon and Gebesee, the measurements of CO_2 fluxes at the field scale were carried out in the framework of the CarboEurope and NitroEurope integrated projects (European Commission Framework VI research programme; Aubinet et al. (2000)). Water vapour and CO_2 fluxes were measured using the eddy covariance method above the crop canopy. Wind speed was monitored with three-dimensional sonic anemometers, and CO_2 concentration with infrared gas analyzers (model Li-7500 at Grignon and model Li-7000 at Gebesee; LiCor Inc., Lincoln, NE, USA) located on a mast above the canopy. Daily net ecosystem carbon dioxide exchanges (g C m^{-2} day^{-1}) were calculated by integrating the 30-minute fluxes determined by the micrometeorological measurements over each day. The gap-filling methodology of CarboEurope-IP was applied to the experimental data sets (Falge et al., 2001). Prior to gap-filling, the gaps in the NEE times series represented 30 and 35 % of the number of total values, at Grignon-PP and Gebesee, respectively. At Rafidin, there were no micrometeorological measurements of CO_2 exchanges.

For the Grignon-PP experiment, N_2O emissions were measured with 6 automatic chambers (55 L, 0.5 m^{-2}) with the method described by Laville et al. (2011). The chambers were sequentially closed for 15 min, resulting in a cycle of 90 min for the six chambers. The N_2O concentrations were measured using an infrared gas analyzer (N_2O Analyzer 46C, Thermo Scientific Inc., Waltham, MA, USA) which was connected on line with the chambers. Air was pumped from the chamber into the gas analyzer and injected back into the chambers after anal-

ysis. Nitrous oxide fluxes were calculated from the slope of the gas concentration increase in the headspace over time. Nitrous oxide emissions were monitored for 442 days from January 1, 2007, to August 31, 2008.

For the three Grignon-PAN plots, the three GHGs (N_2O, CO_2 and CH_4) were measured with 5 static circular chambers (0.2 m^{-2}) per plot. The chambers were closed over a period of 30 minutes and 4 gas samples were collected with a syringe at 0, 10, 20 and 30 minutes after closure. Gas samples were analyzed by gas chromatography fitted with an electron capture detector for N_2O analysis and with a flame ionization detector and a methaniser for CO_2 and CH_4 analysis. From July 2007 to September 2008, eight manual chambers were also deployed in the Grignon-PP field in order to measure N_2O, CO_2 and CH_4 fluxes on a monthly frequency or following fertilizer application. An intensive monitoring of the GHG emissions was carried out following the slurry application in spring 2008 with gas sampling on April 16, 17, 18, 21, 24 and 30.

At Gebesee, GHG measurements were carried out with manual chambers (100×100×30 cm) from February 2006 to December 2007, weekly during the growing season and every two weeks otherwise. The chambers were closed for one hour and sampling was carried out every 20 minutes during closure. Once canopy height exceeded 30 cm, some extensions were fixed on the chambers to include the total canopy. From February to December 2007, two automatic chambers (95×25×125 cm) were installed in the same plot. Gas samples were automatically collected every 20 minutes during one hour of closure and each chamber was closed 6 times in a day. In both cases, gas samples were analyzed with gas chromatography such as described above.

At Rafidin, nitrous oxide emissions were monitored by the static chamber method using circular chambers (0.2 m^{-2}), with 8 replicates on one 30 × 30 m plot for each treatment. On each sampling date, the chambers were closed with an airtight lid, and the head space was sampled 4 times over a period of 2 hours. The gas samples were analyzed in the laboratory by gas chromatography. The measurements were done every 1-3 weeks between September, 1994 and April, 1995

(Gosse et al., 1999).

At the dates of mineral or organic fertilizer application, the chambers were closed during the spreading operation and then, the amount corresponding to the chamber surface was applied by hand within the chambers.

2.2 Indirect GHG emissions

The GHG emissions associated with input production and use of farm machinery were calculated from the Ecoinvent life cycle inventory database (Nemecek et al., 2003). Table 2 summarizes the GHG emissions (CO_2, CH_4 and N_2O) associated with the different inputs, transports and cropping operations. For each crop, specific elementary management operations including soil tillage, fertilization, sowing, plant protection, harvest and transport were translated in terms of GHG emissions based on the emission factors given in the Ecoinvent database. The entire life cycle of each machinery was computed by including the machinery and the tractor production, the production and consumption of diesel and the air emissions during the cropping operations. For fertilizer and pesticides, the production and the transport of the raw materials, the construction of the production plant and the air emissions during manufacturing were included. The final transport stage at the farm included the production of means of transportation, the energy production and consumption and the air emissions were counted in the indirect emissions.

2.3 The CERES-EGC model

CERES-EGC was adapted from the CERES suite of soil-crop models (Jones and Kiniry, 1986), with a focus on the simulation of environmental outputs such nitrate leaching, emissions of N_2O ammonia, and nitric oxide (Gabrielle et al., 2006). The model simulates the cycles of water, carbon and nitrogen within agro-ecosystems (Gabrielle et al., 1995, 2006).

Direct field emissions of CO_2, N_2O, NO and NH_3 into the atmosphere are simulated with differ-

ent trace gas modules (Lehuger et al., 2009, 2010). Here, we focus on gases with global warming potential, i.e. CO_2 and N_2O.

Carbon dioxide exchanges between soil-plant system and the atmosphere are modeled via the net photosynthesis and soil organic carbon (SOC) mineralization processes. Net primary production (NPP) is simulated by the crop growth module while heterotrophic respiration (Rs) is deduced from the SOC mineralization rates calculated by the microbiological sub-model. The net ecosystem production (NEP), which is calculated as NPP minus Rs, may be computed on a daily basis and directly tested against the net ecosystem exchanges measured by eddy covariance (Lehuger et al., 2010).

CERES-EGC simulates the N_2O production in the soil through both the nitrification and the denitrification pathways. The denitrification component calculates the actual denitrification rate (Da, kg N ha^{-1} d^{-1}) as the product of a potential rate at 20 °C (PDR, kg N ha^{-1} d^{-1}) with three unitless factors related to water-filled pore space (F_W), nitrate content (F_N) and temperature (F_T) in the topsoil, as follows:

$$Da = PDR \times F_N \times F_W \times F_T \tag{1}$$

In a similar fashion, the daily nitrification rate (Ni, kg N ha^{-1} d^{-1}) is modeled as the product of a maximum nitrification rate at 20 °C (MNR, kg N ha^{-1} d^{-1}) with three unitless factors related to water-filled pore space (N_W), ammonium concentration (N_N) and temperature (N_T) and expressed as follows:

$$Ni = MNR \times N_N \times N_W \times N_T \tag{2}$$

Nitrous oxide emissions resulting from the two processes are soil-specific proportions of total denitrification and nitrification pathways, and are calculated according to:

$$N_2O = r \times Da + c \times Ni \tag{3}$$

where r is the fraction of denitrified N and c is the fraction of nitrified N that both evolve as N_2O. The N_2O sub-model of CERES-EGC involves a total set of 15 parameters including PDR, MNR, c and r as defined above. The equations of the response functions with the other associated parameters are detailed in Lehuger et al. (2009). CERES-EGC runs on a daily time step and requires input data for agricultural management practices, climatic variables (mean air temperature, daily rain, global radiation and facultatively Penman potential evapotranspiration), and soil properties.

2.4 Parameter selection and model calibration

The parameters of the CO_2 exchange module of CERES-EGC were estimated by Bayesian calibration in a previous study (Lehuger et al., 2010) and we used them for the model simulations of net ecosystem exchanges. A multivariate global sensitivity analysis, developed by Lamboni et al. (2009), allowed us to select the 6 most sensitive parameters of the N_2O emission module of CERES-EGC. The most influent parameters were then estimated with a Bayesian calibration approach. Table 3 recapitulates the parameters involved in the calibration. The calibration was carried out with the N_2O emission measurements of the experimental site of Grignon-PP over the years 2007 and 2008 (340 days of monitoring). The calibrated parameters were then used to simulate the N_2O emission from the Grignon-PAN and Gebesee experiments. The parameters values used for the Rafidin site originated from a previous calibration (Lehuger et al., 2009).

Van Oijen et al. (2005) and Lehuger et al. (2009) described in details the Bayesian method that was used in this work. Briefly, the aim of Bayesian calibration is to reduce the prior parameter uncertainty by using measured data, thereby producing the posterior distribution for the parameters. In our case, we specified lower and upper bounds of the parameterization uncertainty, defining the prior parameter distributions as uniform (Table 3). The posterior probability density function (pdf) is then computed by multiplying the prior pdf with the likelihood function,

which is the data probability given the parameters. Because probability densities may be very small numbers, rounding errors needed to be avoided and all calculations were carried out using logarithms. The logarithm of the data likelihood is thus set up as follows, for each data set Y_i:

$$logL_i = \sum_{j=1}^{K} \left(-0.5 \left(\frac{y_j - f(\omega_i; \theta_i)}{\sigma_j} \right)^2 - 0.5log(2\pi) - log(\sigma_j) \right) \quad (4)$$

where y_j is the mean N_2O flux measured on sampling date j in the data set Y_i and σ_j the standard deviation across the replicates on that date, ω_i is the vector of model input data for the same date, $f(\omega_i; \theta_i)$ is the model simulation of y_j with the parameter vector θ_i, and K is the total number of observation dates in the data sets. To generate a representative sample of parameter vectors from the posterior distribution, we used a Markov Chain Monte Carlo (MCMC) method: the Metropolis-Hastings algorithm (Metropolis et al., 1953). For each calibration, three parallel Markov chains were started from three different starting points in the parameter space (θ_0). Convergence was checked with the diagnostic proposed by Gelman and Rubin (1992). The chains were considered to be a representative sample from the posterior pdf, and the mean vector, the variance matrix and the 90% confident interval of each parameter were calculated.

2.5 Model evaluation

Two statistical indicators were used to evaluate the model's goodness of fit to observed data: the mean deviation (MD) defined as:

$$MD = \frac{1}{K} \sum_{j=1}^{K} (y_j - f(\omega_k; \theta_l)) \quad (5)$$

and the root-mean squared error (RMSE) calculated as:

$$RMSE = \sqrt{\frac{1}{K} \sum_{j=1}^{K} (y_j - f(\omega_k; \theta_l))^2} \quad (6)$$

where y_j is the time series of the observed data on day j of data set D_i, and f($\omega_k; \theta_l$) is the corresponding model predictions with input variables ω_k and parameters θ_l.

The RMSE was computed for the experiments used in the calibration (Grignon-PP and Rafidin) and in the subsequent model testing against the independent data sets of Grignon-PANs, and Gebesee. In both last cases, the RMSE corresponds to the root mean square error of prediction (RMSEP(θ)), since the data were involved neither in parameter estimation nor model development (Wallach, 2006). The RMSEP was computed for the predictions of N_2O emissions.

2.6 Net greenhouse gas emissions of crop rotations

The carbon balance was calculated as the net biome production (NBP) equal to:

$$NBP = NEP - Exported\,biomass + Imported\,biomass \quad (7)$$

The NEP is the net ecosystem production and corresponds to the net C exchanges between agro-ecosystems and the atmosphere. Exported biomass corresponds to harvested products and imported biomass to the applications of manure or compost. The carbon dioxide exchange for a crop was accumulated from its sowing to the sowing of the following crop. The values of NBP were obtained by averaging the NBP simulated over 12 maize-wheat-barley-mustard rotations on a 36-yr series of historical weather data (1972-2008) for Grignon-PP, with constant crop management corresponding to the real practices of the 2005-2007 crop sequence (Table 1). The same simulation was done for the three treatments of Rafidin over 9 rapeseed-winter wheat-winter barley rotations on a 27-yr series of weather data with constant crop management corresponding to the practices over the 1994-1997 time period (Table 1). Simulating the rotations over about 30 years allowed us to explore the climatic variability and its effect on the net primary production and soil respiration. For Grignon-PANs and Gebesee simulations, the model was run for two rotations before the measurement period to stabilize the C and N soil pools and dampen the initial conditions and only the last rotation was used to compute the GHG balances.

The net greenhouse gas balance of crop sequences was computed by adding model predictions of NBP and N_2O emissions, measurements of CH_4 exchanges in the case of Grignon-PP and

the indirect emissions. Global warming potential of the GHGs were used at the 100-year time horizon (CO_2=1, CH_4=25 and N_2O=298 ; IPCC (2007)). The usual sign convention for NBP is that a positive NBP corresponds to a net carbon fixation, but we reversed it in the calculation of the net GHG balance. Methane fluxes were ignored to compute the GHG balance of Rafidin rotation due to a lack of measurement for this gas at this site. The GHG balances were expressed in kg CO_2-C equivalent using the mass conversion factor of 12/44 kg C/kg CO_2.

2.7 Mitigation scenarios

Five scenarios were tested in order to assess the effect of agricultural practices on the net GHG balance, and to explore the potential of GHG abatement at cropping systems level. They were implemented based on the Grignon-PP rotation, with a 36-year simulation time period. The first scenario (*SW*) was designed to assess the effect of returning straw to the soil rather than removing it. The scenario (*CC*) compared rotations with and without a catch crop, in this case a mustard was grown between the harvest of a winter crop and the sowing of a spring crop. We also tested the effect of N fertilization rates by simulating rotations with either 50% less (scenario *N*-) or 50% more (scenario *N*+) N inputs compared to the baseline management. The last scenario (*ORG*) was run to evaluate the effect of the absence of C and N input from slurry application on the GHG balance of the rotation compared to the baseline management with a slurry application after barley every three years.

3 Results

3.1 Model testing

3.1.1 Crop growth

At Grignon, the crop growth was well simulated for the various crop species of the rotation, as reported in Fig. 1.a. The maize silage yield was underestimated in 2005 with bias (observed -

simulated yields) of 1960 kg DM ha^{-1}, due to too high water stress simulated but the maize yield was well simulated in 2008. The grain yields of barley and winter wheat were predicted with discrepancies of -100 and -430 kg DM ha^{-1}, between simulations and observations. The LAI increase and the senescence phase were well simulated with a RMSE of 1.37 m^2 m^{-2} over the period 2005-2008 (Fig.1.b).

At the Rafidin site, CERES-EGC provided good simulations of rapeseed growth for the N1 and N2 treatments. The simulated patterns of biomass (Fig. 2a, d), LAI (Fig. 2b, e) and N content (Fig. 2c, f) variations matched the observations over the entire growing cycles. Final grain yields were well estimated, with a simulated value of 3.8 t DM ha^{-1} and an observed one of 4.1 t DM ha^{-1} for N1, and an exact match at 4.9 t DM ha^{-1} for N2. The root mean square errors of the simulated LAI against the measured LAI were 0.7 and 0.5 m^2 m^{-2} for the rapeseed crop of the N1 and N2 treatments respectively. For the N0 treatment (unfertilized), the model overestimated LAI by a factor of 2 throughout the growing season, but total above ground biomass was underestimated by about 25% when compared to the data (not shown). For this treatment, the simulated N stress was too high at the end of the crop's growing cycle to allow sufficient grain filling, and the final grain yield was underestimated as a result.

3.1.2 Net carbon exchanges

The carbon dioxide exchanges measured by eddy covariance were used either to calibrate the model parameters or to evaluate the model prediction accuracy (Lehuger et al., 2010). The measurements from Grignon-PP were used for the parameter estimation and those of Gebesee for evaluation of the model prediction accuracy. For both sites, NEP was well simulated at daily and seasonal scales (Fig. 1.c and Fig. 3). The RMSE computed for the Grignon-PP experiment was 1.90 g C $m^{-2}d^{-1}$ (n=1627) and the RMSEP of Gebesee 1.5 g C $m^{-2}d^{-1}$ (n=310). The RMSE of cumulative sum of NEP was 137.65 g C m^{-2} over the 2005-2008 maize-wheat-barley-mustard

rotation at Grignon-PP and 90.95 g C m^{-2} over the 2007 winter wheat crop cycle at Gebesee.

3.1.3 Soil drivers of N_2O emissions

Figure 4 provides a test for the simulation of the key drivers of N_2O emissions at the Grignon-PP site. Soil moisture, temperature and inorganic N content control N_2O emissions by their influence on the nitrification and denitrification processes. At Grignon, for the period of measurement (2006-2008), their dynamics were well predicted (Fig. 4.a, 4.b, 4.c), except for soil water content which was slightly underestimated during summer periods in 2007 and 2008. Table 4 recapitulates the MDs and RMSEs computed with the different soil drivers used as input variables of the N_2O emission module. Soil temperature and soil water content were well predicted by the model with RMSE close to 3°C for the soil temperature and from 4 to 8% (v/v) for the soil water content across the field-site experiments. The model's RMSE over the 8 experiments ranged between 9.9 and 57.0 kg N ha^{-1} for the simulation of nitrate content and to 4.1 to 28.6 kg N ha^{-1} for the ammonium content. For the Grignon-PAN2 field site, the model did not fit with the measurements of NO_3^- and NH_4^+ soil contents. An over-application of nitrogen due to wrong settings of the fertilizer spreader in this plot could explain the high N amount in soil and the lack of correlation between measured N concentration values and recorded N fertilizer supplies in this plot.

3.2 Nitrous oxide emissions

The three parallel chains that were run for the Bayesian calibration against Grignon-PP site, converged well for all the parameters after 50 000 iterations. Table 3 summarizes the posterior expectancy of parameters, their standard deviation and their correlations with other parameters. The posterior ratio of N_2O to total denitrification was higher than its default value, while the posterior potential denitrification rate was highly reduced, down to 0.33 compared to a default value of 6.00 kg N ha^{-1} d^{-1}. On the other hand, the posterior value of the WFPS threshold for denitrification, the half-saturation constant for denitrification and the temperature threshold

remained close to their default values.

Fig. 5 compares the simulations of daily N_2O emissions after calibration and the observations of the Grignon-PP experiment. There was good agreement between simulated and observed data during the mineralization of crop residues of the barley in 2007. The RMSE between simulated and measured data for the period from 19 Jul. 2007 to 23 Jan. 2008 was 7.6 g N_2O-N ha^{-1} d^{-1} (n=183 and mean of measured data=7.0 g N_2O-N ha^{-1} d^{-1}). The first measured emission peak in March 2007, corresponding to the first N fertilizer application, was not captured by the model due to simulated WFPS remaining under 61% - the threshold that triggers denitrification in the model. The high fluxes that occurred in spring 2008 consecutive to the slurry and N-fertilizer applications for maize were well predicted. The subsequent observed N_2O emissions were low and the model simulated emissions close to zero. The RMSE obtained with the complete measured data set and the posterior expectancy of parameters was 30% less than with the default parameter values, evidencing the benefits of the calibration (Table 5).

Fig. 6 shows the dynamics of N_2O emissions for the three treatments of the Rafidin sites. Observed N_2O emissions were very low even for the high-N input treatment (N2). In fact, for this treatment, the highest emission rate measured was 7.4 g N_2O-N ha^{-1} d^{-1}. At this site, the rates of N_2O emissions from denitrification were close to zero. Hénault et al. (2005) estimated that 98% of the N_2O emissions originated from the nitrification process at the same Rafidin site. The predicted rates of N_2O emissions were satisfactory, with RMSEs of 0.3, 1.4 and 3.0 g N_2O-N ha^{-1} d^{-1} after calibration for the N0, N1 and N2 treatments respectively (Table 5).

The calibrated model was used to simulate the experiments of Grignon-PAN1,-PAN2 and -PAN3 and of Gebesee. We could thus assessed the model prediction error via the calculation of the RMSEP, as reported in Table 5. Values of RMSEP were lower with the calibrated parameter set compared to the default one, by 6.3% in average for the Grignon-PAN1, -PAN2, -PAN3 treatments and by 39% for Gebesee experiment. Fig. 7 depicts the N_2O emissions over one year for

the three treatments PAN1, PAN2 and PAN3 of the Grignon site and shows that the model predicts the N_2O emission peaks subsequent to the N-fertilizer application that occurred in spring 2008, and also the period of low emissions ensuing.

Fig. 8 shows the time course of N_2O emissions at Gebesee. The low emissions and the largest N_2O peaks occurring in Sept-Oct 2007 at this site were predicted by the model.

3.3 Simulation of crop rotations

In the previous section, we tested and calibrated the CERES-EGC model against datasets from 8 field site experiments involving different sets of crop types, pedoclimatic conditions, and agricultural practices. In the present section, we used the model to calculate the GHG balance of complete crop rotations, including net C exchanges, direct emissions of N_2O and CH_4 fluxes in the field, and indirect (upstream) emissions.

3.3.1 Net biome production

Fig. 9 displays the breakdown of the NBP for the Grignon-PP rotation. The net ecosystem production values were 5828$\pm$890 kg C ha^{-1}, 5301$\pm$750 and 4778$\pm$634 kg C ha^{-1} for maize, wheat and barley, respectively. For the mustard, the soil respiration term was greater than net photosynthesis, and NEP was thus negative at -441$\pm$68 kg C ha^{-1} (Table 6). At Rafidin, the NEP of rapeseed was 1303$\pm$1420, 4263$\pm$995 and 4639$\pm$1168 kg C ha^{-1} for the N0, N1 and N2 treatments, respectively (Table 6). The NEP of wheat ranged between 4877 and 5194 and the NEP of barley between 3149 and 3440 kg C ha^{-1} (Table 6). Inter-annual variability was quite large for the net primary production (Fig.9),pinpointing the strong dependency of crop growth on climate. The coefficient of variation (CV, ratio of the SD to the mean) was 11% on average for the maize, wheat and barley crops.

Over the 36-yr simulation periods with the maize-wheat-barley-mustard rotation in Grignon-PP, we estimated a stable soil organic C (SOC) stock with a slight loss of 10 kg C ha^{-1} yr^{-1}. At

Rafidin, we estimated large SOC accumulation rates amounting to 525, 1153 and 1269 kg C ha^{-1} yr^{-1} for the N0, N1 and N2 treatments, respectively. This arised in part because of the lower fraction of net primary production which was exported out of the field, compared to Grignon-PP. At Grignon, the straw of wheat and barley was removed for use as animal litter, whereas at Rafidin the straw was left on the soil surface at harvest, and subsequently incorporated into the topsoil. As a consequence, the C inputs from crop residues were much higher at Rafidin than at Grignon, averaging 4250 kg C ha^{-1} yr^{-1} for the N1 rotation and 4290 kg C ha^{-1} yr^{-1} for the N2 rotation (Table 6). With these levels of C inputs to the soil, the CERES-EGC model predicted a high C sequestration for the rotations of Rafidin suggesting that the Rafidin soil was a potentially large sink for atmospheric CO_2.

For the other experimental fields of Grignon, the NBPs were -85 for the PAN1 treatment, 256 for the PAN2 treatment and -32 kg C ha^{-1} yr^{-1} for the PAN3 treatment (Table 7). Despite its largest NEE, the NBP of Grignon-PAN2 was higher than those of Grignon-PAN1 and -PAN3 due to its large maize exports in 2007. At Gebesee, the NEE and exports of wheat crop cycle were half of the averaged NEE and exports of the Grignon-PANs, but the large amount of C from manure and slurry applications made the NBP very low at this site.

3.3.2 Indirect emissions

The GHG of agricultural inputs contributes a large part of the GHG balance of agro-ecosystems. For the Grignon-PP cropping system, the mean IE were 350 kg CO_2-C eq ha^{-1} yr^{-1} which represented half of the GHG balance. For the Rafidin system, the mean IE were 320, 410 and 460 kg CO_2-C eq ha^{-1} yr^{-1} for the N0, N1 and N2 treatments, respectively (Table 6). For the Grignon-PAN treatments, the mean IE were 420, 480 and 410 kg CO_2-C eq ha^{-1} yr^{-1} for PAN1, PAN2, PAN3 treatments, respectively. The IE were 589 kg CO_2-C eq ha^{-1} yr^{-1} for the wheat crop cycle of Gebesee, a higher value compared to the other site due to more frequent cropping

operations(Table 7). N fertilizer production is the top contributor to the IE by a wide margin, with a 55-75% share (Fig. 10). Cropping operations came next, with a 30-40% in the total IE term, mainly due to fossil-fuel combustion by farm machinery. The transport of inputs from the production plant to the farm was the lowest contributor to the GHG balance with less than 1% of IE.

3.4 Net greenhouse gas balance

The simulation of rotations enabled us to explore the effect of climate variability on biomass production and N_2O emissions. At Grignon-PP, N_2O emissions averaged 316$\pm$61 kg CO_2-C eq ha^{-1} yr^{-1} (CV=20%) over maize-wheat-barley-mustard rotation, and we estimated a GHG balance of 2011 kg CO_2-C eq ha^{-1} over the full rotation or 670$\pm$226 kg CO_2-C eq ha^{-1} per year on average (Table 6) for this system. Methane measurements from manual chambers allowed us to estimate its contribution to the final GHG balance. The Grignon soil was a weak methane sink which mitigated the GHG balance of the rotation by only 2%.

At Rafidin, we estimated three times lower N_2O emissions than at Grignon-PP ($<$140 kg CO_2-C eq ha^{-1} yr^{-1}), and a large C storage potential resulting from the high level of residue return that offset the emissions of N_2O and the indirect emissions. The GHG balances were -90$\pm$624, -621$\pm$660 and -673$\pm$723 kg CO_2-C eq ha^{-1} yr^{-1} for the N0, N1 and N2 systems, respectively (Table 6). The Rafidin crop rotation is an intensive system with a high level of inputs and indirect emissions of GHG, but it is compensated for by the resulting high potential of biomass production and SOC storage. Overall, the Rafidin system emerges a potentially strong sink of GHG.

The Table 7 summarizes the GHG balances for the PAN1, PAN2, PAN3 treatments of Grignon and that of the wheat crop cycle of Gebesee. For each field site, only one crop sequence was simulated. The Grignon-PANs experiments had the same crop sequences as Grignon-PP but without slurry application and maize was harvested for grain and not for silage as it was the case

at Grignon-PP. The PAN1, PAN2 and PAN3 treatments were net sources of GHGs with 509, 913 and 547 kg CO_2-C eq ha^{-1} yr^{-1}, respectively. The net GHG balance was higher in the PAN2 treatment due to an additional N fertilizer application on wheat in comparison with the two other treatments. At Gebesee, the wheat crop cycle was a high sink of GHGs due to high C input from manure and slurry applications during its cropping cycle.

Figure 11 shows the ratio between net GHG balance and kg C exported (GHG intensity) for each crop of the different treatments. The GHG intensities were all lower than 1 meaning that the net GHG balance in C-eq were all lower than the C exports (Fig. 11). In some cases the ratio can be below 0 meaning that the crop had fixed more C than the sum of all the GHG emissions plus the C exports. The maize crop in Grignon-PAN1 and -PAN3 had the lowest GHG intensities due to a large return of crop residues to the soil. The GHG intensity of maize in Grignon-PP was slightly higher than 0 due to an export of the complete plant for silage. The highest GHG intensities were those of the wheat crop of the 3 Grignon-PAN treatments with a mean value of 0.41 kg CO_2-C kg^{-1} C exported followed by the Grignon-PP with a value of 0.25 and those of Rafidin treatments with a mean value of -0.24. The additional N fertilizer application in the Grignon-PAN2 treatment led to a higher GHG intensity compared to Grignon-PAN1 and Grignon-PAN3 (0.46 vs 0.37 an 0.39 kg CO_2-C kg^{-1} C exported respectively). It did not lead to an extra C fixation and higher yield that compensated the additional indirect and direct emissions. While the management of the barley crop was quite different between the treatments (Table 1) the GHG intensities were quite homogeneous and ranged between 0.06 and 0.21. The GHG intensities of rapeseed crop from Rafidin N1 and Rafidin N2 are quite similar. The largest GHG emissions of the N2 treatments are compensated by a larger crop productivity and return of crop residues compared to the N1 treatment. The variability of the GHG intensity within the crop species was high suggesting that ascribing a unique value per crop was not possible if the management and pedoclimatic conditions were not taken into account.

3.5 Mitigation strategies

Figure 12 compares the net GHG balance of five scenarios with differentiated management crop practices. The initial (baseline) scenario was the cropping system of Grignon-PP, as described in section 2.7. Scenario *SW* with straw returned to the soil had the lowest GHG balance due to a high negative CO_2 balance. Despite of a substantial increase of soil respiration (+50% compared to the initial scenario), the return of C from crop residues increased the SOC by 265 kg C ha^{-1} yr^{-1} and reduced the GHG balance by 35% compared to the baseline.

The effect of not planting the mustard catch crop between barley and maize was negligible compared to the initial scenario. This was due to a very low C fixation simulated in the initial scenario and the C input from slurry application, that made mustard a strong C sink, was attributed to the previous barley crop in this scenario.

Nitrogen fertilization affects the GHG balance due to its effects on C fixation, N_2O emissions and indirect emissions. Increasing the amount of mineral N fertilizers by 50% involved a GHG balance 22% higher than that of the initial scenario for which the N fertilization was balanced in relation to N crop demand. N_2O emissions were increased by 17%, indirect emissions by 27% and net primary production only by 1% meaning that optimal yield was already reached with fertilization in the initial scenario. On the contrary, decreasing the N fertilizer by 50% led to a 27% decrease of GHG balance compared to the initial scenario.

We assessed in the last scenario, the effect of slurry application on the GHG balance. Organic fertilizer application represented large inputs of C and N inputs to the agro-ecosystem, and its elimination of the rotation resulted in a 45% higher GHG balance but in a reduction of 20% of the N_2O emissions in comparison with initial scenario. Slurry added in the crop system 1760 kg C ha^{-1} which represented half of the C exported by straw removal.

The GHG intensities were 0.12, 0.09, 0.12, 0.14, 0.09 and 0.17 kg CO_2-C eq kg C^{-1} for the *I*, *SW*, *CC*, *N+*, *N-* and *ORG* scenarios for the entire rotations, respectively (data not shown).

The worst option was the removal of organic fertilizer in the rotation followed by the option of increasing N fertilizer rate by 50%. Decreasing N fertilizer rate by 50% led to a similar GHG intensity as the option of straw incorporation in soil with a reduction of around 20% of the GHG intensity compared to the baseline scenario.

4 Discussion

4.1 Relevance of modeling to the estimation of GHG balances

The first objective of this work was to test and calibrate the CERES-EGC model against experimental data of CO_2, N_2O, soil variables and crop biomass, from 3 temperate sites located in Western Europe. The model adequately captured the time course of total above-ground biomass for the crops of the rotations (maize, wheat, barley, rapeseed), along with the net carbon exchanges between the soil-plant system and the atmosphere from daily to growing season and crop rotation time scales. The soils drivers for N_2O emissions were correctly predicted for all sites except at Grignon-PAN2 where N soil content measurements were not in agreement with the amount of N applied. Accordingly, N_2O emissions were in agreement with the observations in all sites with RMSEs or RMSEPs computed with the calibrated model that ranged between 0.3 to 14.2 g N_2O-N ha^{-1} d^{-1}. At Grignon-PP, the underestimation of SWC during the driest periods in summer did not lead to model error of N_2O emissions because denitrification was inactivated by the low WFPS which was below the activation threshold parameter of the denitrification process. Applying Bayesian calibration to the six most influent parameters of the nitrous oxide emission module allowed us to reduce error of prediction by 6-40% compared to default parameters-based simulations against 4 independent data sets of N_2O measurements. The mean RMSEP of N_2O emissions for the 4 treatments of model validation (Grignon-PAN1, -PAN2, -PAN3 and Gebesee) was estimated to 200% relatively to the daily mean of measured N_2O fluxes. The uncertainty of model simulation at daily scale was quite high but the propagation of this normal error of stan-

dard deviation 200% times the daily N_2O flux in the calculation of the accumulated N_2O budget over the full rotation, led to an error of 10% around the simulated annual mean (i.e. 95 kg CO_2-C eq for the full rotation). Hence the uncertainty on the accumulated N_2O flux was low enough to allow us the comparison between different mitigation scenarios.

The model was not designed to simulate neither the N_2O consumption by soil surface nor the N_2O production after freeze-thawing. Few field studies have shown and explained the denitrification dynamics for these types of processes (Neftel et al., 2007). The mechanisms are still not very well-known and it is still difficult to formalize the soil processes in our model. Several hypotheses which are reported in Laville et al. (2011) may explain the fluxes during freeze-thaw periods and only few models are able to estimate the net N_2O emissions, e.g. de Bruijn et al. (2009) tested different hypotheses with the MOBILE model and Grant and Pattey (1999) incorporated the mechanisms in the Ecosys model. The inability of CERES-EGC to simulate the mechanisms may lead to overestimation of the net emissions in areas with stronger continental influences and frequent freeze-thawing but the effects of such processes were of relatively low magnitude at Grignon, and neither was noted at Rafidin (Hénault et al., 2005). However, the model can not predict the N_2O deposition and N_2O emissions due to freeze-thaw periods that were observed at the Gebesee site.

Other studies with similar modeling approaches report discrepancies between modeled and observed N_2O data in a similar range as our simulations. Del Grosso et al. (2008) reported that DAYCENT largely overestimated N_2O emissions in irrigated system -daily R^2 were less than 2%- due to an over responsive effect of soil NO_3^- on N_2O. In the same way, Babu et al. (2006) indicate that the DNDC model predicted daily N_2O fluxes with a large lack of fit (RMSE = 529.6 g N_2O-N ha^{-1} d^{-1}, n=134) for rice-based production systems in India with high level of N_2O emissions (observed daily mean=49.4 g N_2O-N ha^{-1} d^{-1}). Frolking et al. (1998) and Li et al. (2005b) compared different models or sub-models for their aptitude to simulate N_2O emissions from crop-

land, and in most cases, the models were not able to capture the N_2O flux dynamics because of temporal deviation of the fluxes, time lag between observed and modeled peaks and over- or underestimation of the measured N_2O peaks.

Regarding the C balance, we assumed that the budget between the net ecosystem production, the organic C exported by harvesting and imported by manure reflected the SOC changes. The C-budget of the Grignon-PP field-site was nearly balanced, while Rafidin had a high potential of C sequestration resulting from a high C fixation by crops and a large fraction of inputs as crop residues due to no straw exports. As a consequence, the SOC storage was estimated between 500 and 1300 kg C ha^{-1} yr^{-1} for the various treatments at Rafidin. This result is in agreement with the relatively low SOC mineralization rate of rendzina soils ($<$0.5% of SOC yr^{-1}), such as that of Rafidin, due to physical protection process by the formation of calcite on the organic fractions (Trinsoutrot et al., 2000). Thus, the high level of biomass production permitted by ample fertilizer inputs, together with this low SOC mineralization rate induced a large net fixation of atmospheric CO_2. Adviento-Borbe et al. (2007) measured the SOC changes over a 5-yr period in continuous maize system with recommended and intensive fertilization treatments (+70-100% more N fertilizer applied than in the recommended treatment) in Nebraska (USA). They reported SOC sequestration rates of 440 and 620 kg C ha^{-1} yr^{-1} for the recommended and intensive treatments, respectively, mainly due to high C residue from maize crops which ranged between 5500 and 6500 kg C ha^{-1} yr^{-1} in both systems. At Rafidin, SOC accumulation for the intensive rotation was almost twice greater than those of the intensive treatment reported by Adviento-Borbe et al. (2007) whereas inputs from crop residues were slightly lower.

The C dynamics predicted by the model were evaluated at the daily time scale against micrometeorological measurements of CO_2 exchanges for entire crop rotations, but it will be necessary to supplement this test by further verifying the ability of CERES-EGC to simulate the rate of soil C changes in the long term.

4.2 Model application for predicting net GHG balance

Applying the model to predict the GHG balance of crop rotations was the second objective of this work. The GHG balances of Rafidin and Grignon-PP were markedly different: the rapeseed-wheat-barley rotation on a rendzina was a net sink of GHG with a GHG balance of -620 to -670 kg C ha^{-1} yr^{-1} for the N1 and N2 treatments, respectively, while the maize-wheat-barley-mustard rotation on a loamy soil at Grignon was a net source of GHG, with a balance of 670 kg C ha^{-1} yr^{-1}. The main difference between both sites was from the management of the crop residues and its effect on the variation of SOC. In addition, the soil type at Rafidin minimized the N_2O emissions due to its soil specific parameters that inhibited the denitrification process (Hénault et al., 2005). Hence the N_2O flux at Rafidin N1 was 2.5 times lower than that of Grignon-PP whereas the IE were only 15% lower for the rotation of Grignon-PP.

Our results were within the range of GHG balances reported by Ceschia et al. (2010) who computed GHG balances of 15 cropland sites in Europe based on eddy covariance CO_2 flux measurements. The study sites were sources of GHG by 1900$\pm$2570 kg C-eq ha^{-1} yr^{-1} on average. Their estimation for the Grignon-PP site was 3590 kg C-eq $ha^{-1}yr^{-1}$ by including only winter wheat and barley crops during the period 2006-2007. While their evaluation of N_2O emissions and indirect emissions were 44% (176 vs. 316 kg C-eq ha^{-1} yr^{-1}) and 37% (220 vs. 347 kg C-eq ha^{-1} yr^{-1}) lower, respectively, than our estimates, the net C balances were 5 and 4 times higher than our values for wheat and barley, respectively. Their values of cumulated indirect and N_2O emissions represented 10% of the GHG balance on average whereas we estimated that the IE and N_2O emissions each contributed half of the emission sources at Grignon-PP. The differences with their results were from (i) the methods used to estimate, NBP, IE and N_2O emissions and (ii) the system boundaries for IE. They used IPCC emission factors to estimate N_2O emissions and a compilation of literature data for IE, whereas we used the CERES-EGC model and a LCA database, respectively.

4.3 Efficiency of mitigation options

The last objective of this work was to assess the sensitivity of GHG balances to different agricultural mitigation practices. The most efficient strategy we identified was to keep the crop residues in the system without exporting the straw produced by wheat and barley crops. The scenario *SW* had also the lowest GHG intensity: 0.09 kg C eq kg^{-1} C exported against 0.12 kg C eq kg^{-1} C exported for the initial scenario. Laville et al. (2011) showed that the mineralization of organic matter by incorporation of crop residues was found to be one of the main factor controlling the N_2O emissions peaks at the Grignon-PP site. The authors estimated that between August and December 2007, the accumulated N_2O emissions over the 5 months totaled 56% of the annual emission although no N was applied during this period. In our case, while the mineralization of crop residues and soil organic matter after the harvest led to substantial N_2O emission peaks, it was not high enough to offset the beneficial effects of the C return.

The worst option consisted of removing the organic fertilizer application which provided a substantial input of C for the entire crop rotation. The simultaneous decrease of N supply in the system did not lead to significant reduction of N_2O emissions which could have compensated the C loss. The GHG intensity of this scenario is also the worst with a value of 0.17 kg C eq kg^{-1} C exported. The GHG intensity was related to the total C exported from the field without distinguishing either the crop type, its intrinsic quality (e.g. the protein grain content) or its function (e.g. biomass for food, feed, litter bedding, bioenergy...). Thus, our GHG intensity values can not be used as emission factors for LCA inventories (Ceschia et al., 2010).

Reducing N fertilizers implies lower N_2O and indirect emissions but C fixation by plant is also reduced and, as a result, the supply of fresh organic matter supply to soil is diminished. For the Rafidin site, the most intensive system (N2) was the system with the lowest GHG balance due to a large capacity to store C fixed by crops, whereas, adding a third N fertilizer split application on the wheat crop in the rotation of the Grignon-PAN2 treatment resulted in a greater GHG balance

due to higher indirect and N_2O emissions not being compensated for by the limited benefit in term of C fixation. This extra application was actually aimed at increasing the protein grain content, i.e. the economic value of the harvest, and not crop biomass. In the same way, the scenario *N+* applied at Grignon-PP led to a low increase in NEP which did not compensate the increase in N_2O and IE emissions and its GHG intensity was 17% higher than that of the initial scenario. On the contrary, the scenario *N-* had a GHG intensity 25% lower than the initial scenario meaning that reducing the N supply implied a strong effect on IE and N_2O emissions without degrading the NEP and the yield.

5 Conclusion

The assessment of the direct emissions at the field scale is paramount to an accurate estimation of GHG balances for agricultural systems. Biophysical modeling of the soil-crop-atmosphere system provides a unique capacity to address this issue while taking into account the complex interactions between C and N cycling, as influenced by anthropogenic actions. Here, we tested and calibrated the CERES-EGC model to simulate the GHG fluxes of the agro-ecosystem, and showed it achieved satisfactory predictions of N_2O and CO_2 fluxes for different cropping systems representing distinct pedoclimatic conditions and agricultural practices.

The C dynamics predicted by the model were validated at the daily time scale against micrometeorological measurements of CO_2 exchanges in two of the three sites, but it will be necessary to supplement this test by further verifying the ability of CERES-EGC to simulate the rate of changes in the long term (Gabrielle et al., 2002).

The modeling approach was used to devise different strategies to mitigate the GHG balance of cropping systems. Various scenarios involving some modifications of crop management (e.g., fertilization, rotation, crop residue management) were tested for this purpose. Assessing the effects of new mitigation strategies requires an integrative system approach in order to consider

the whole ecosystem functioning that encompasses the indirect effects of mitigation strategies and counter-intuitive or unintentional flux changes (Robertson and Grace, 2004). Implementation of mitigation strategies that combines simultaneously the options of i) enhancing soil carbon sequestration, ii) reducing N_2O emissions and iii) minimizing synthetic fertilizer use would be highly efficient in term of systemic reduction of GHG balance. Although the CERES-EGC model allowed us to quantify GHG balance of cropping systems and to test some mitigation strategies, it faced with a number of limitations in that it lacks a capacity to i) fully account for the effect of tillage practices on the soil C changes, ii) reflect the nitrification inhibitor effects on N_2O emissions and iii) simulate methanogenesis and methanotrophy processes in soil and the resulting CH_4 fluxes. Further developments should focus on these points to improve the accuracy of GHG balance quantification and the assessment of mitigation options and new mitigation technologies. Other environmental impacts may also be output by the model and included in the analysis, in particular the emissions into air and water of NH_3, NO_3^-, and NO. Thus, the overall environmental balance of the agricultural systems may be approached, making it possible to design agricultural systems with high environmental performance.

Acknowledgements

This work was part of the CarboEurope and NitroEurope Integrated Projects (EU's Sixth Framework Programme for Research and Technological Development), which both investigate the European terrestrial greenhouse gas balance. We express special thanks to Christophe Fléchard (INRA, Rennes) for its assistance in the analysis of gas sampling and to Annette Freibauer and Werner L. Kutsch (Max Plank Institute, Jena) for making the data from Gebesee available. We would also like to thank the two anonymous reviewers for their valuable comments and suggestions.

References

Adler, P. R., Del Grosso, S. J., and Parton, W. J., 2007. Life-cycle assessment of net greenhouse-gas flux for bioenergy cropping systems. Ecol. Appl. 17, 675–691.

Adviento-Borbe, M. A. A., Haddix, M. L., Binder, D. L., Walters, D. T., and Dobermann, A., 2007. Soil greenhouse gas fluxes and global warming potential in four high-yielding maize systems. Glob. Change Biol. 13, 1972–1988.

Ammann, C., Flechard, C. R., Leifeld, J., Neftel, A., and Fuhrer, J., 2007. The carbon budget of newly established temperate grassland depends on management intensity. Agr. Ecosyst. Environ. 121, 5–20.

Anthoni, P. M., Knohl, A., Rebmann, C., Freibauer, A., Mund, M., Ziegler, W., Kolle, O., and Schulze, E. D., 2004. Forest and agricultural land-use-dependent CO_2 exchange in Thuringia, Germany. Glob. Change Biol. 10, 2005–2019.

Arrouays, D., Balesdent, J., Germon, J. C., Jayet, P. A., Soussana, J. F., and Stengel, P., 2002. Stocker du carbone dans les sols agricoles de France?. Expertise scientifique collective. INRA, Paris.

Aubinet, M., Grelle, A., Ibrom, A., Rannik, U., Moncrieff, J., Foken, T., Kowalski, A. S., Martin, P. H., Berbigier, P., Bernhofer, C., Clement, R., Elbers, J., Granier, A., Grunwald, T., Morgenstern, K., Pilegaard, K., Rebmann, C., Snijders, W., Valentini, R., and Vesala, T., 2000. Estimates of the annual net carbon and water exchange of forests: The EUROFLUX methodology. Adv. Ecol. Res. 30, 113–175.

Babu, Y. J., Li, C., Frolking, S., Nayak, D. R., and Adhya, T. K., 2006. Field validation of

DNDC model for methane and nitrous oxide emissions from rice-based production systems of India. Nutr. Cycl. Agroecosys. 74, 157–174.

Bhatia, A., Pathak, H., Jain, N., Singh, P. K., and Singh, A. K., 2005. Global warming potential of manure amended soils under rice-wheat system in the Indo-Gangetic plains. Atmos. Environ. 39, 6976–6984.

Boote, K. J., Jones, J. W., and Pickering, N. B., 1996. Potential uses and limitations of crop models. Agron. J. 88, 704–716.

Ceschia, E., Béziat, P., Dejoux, J. F., Aubinet, M., Bernhofer, C., Bodson, B., Buchmann, N., Carrara, A., Cellier, P., Di Tomasi, P., Elbers, J. A., Eugster, W., Grünwald, T., Jacob, C. M. J., Jans, W. W. P., Jones, M., Kutsch, W., Lanigan, G., Magliulo, E., Marloie, O., Moors, E. J., Moureaux, C., Olioso, A., Osborne, B., Sanz, M. J., Saunders, M., Smith, P., Soegaard, H., and Wattenbach, M., 2010. Management effects on net ecosystem carbon and GHG budgets at European crop sites. Agr. Ecosyst. Environ. 139, 363–383.

Conrad, R., 1996. Soil microorganisms as controllers of atmospheric trace gases (H_2, CO, CH_4, OCS, N_2O, and NO). Microbiol. Rev. 60, 609–640.

de Bruijn, A.M.G., Butterbach-Bahl, K., Blagodatsky, S., Grote, R., 2009 Model evaluation of different mechanisms driving freeze-thaw N_2O emissions.. Agr. Ecosyst. Environ. 133, 196-207.

Del Grosso, S. J., Halvorson, A., and Parton, W., 2008. Testing DAYCENT model simulations of corn yields and nitrous oxide emissions in irrigated tillage systems in Colorado. J. of Environ. Qual. 37, 1383–1389.

Del Grosso, S. J., Mosier, A. R., Parton, W. J., and Ojima, D. S., 2005. DAYCENT model

analysis of past and contemporary soil N_2O and net greenhouse gas flux for major crops in the USA. Soil Till. Res. 83, 9–24.

Desjardins, R. L., Smith, W., Grant, B., Campbell, C., and Riznek, R., 2005. Management strategies to sequester carbon in agricultural soils and to mitigate greenhouse gas emissions. Climatic Change 70, 283–297.

Falge, E., Baldocchi, D., Olson, R., Anthoni, P., Aubinet, M., Bernhofer, C., Burba, G., Ceulemans, G., Clement, R., Dolman, H., Granier, A., Gross, P., Grunwald, T., Hollinger, D., Jensen, N. O., Katul, G., Keronen, P., Kowalski, A., Lai, C. T., Law, B. E., Meyers, T., Moncrieff, J., Moors, E., Munger, J. W., Pilegaard, K., Rannik, U., Rebmann, C., Suyker, A., Tenhunen, J., Tu, K., Verma, S., Vesala, T., Wilson, K., and Wofsy, S., 2001. Gap filling strategies for long term energy flux data sets. Agr. and Forest Meteorol. 107, 71–77.

Frolking, S. E., Mosier, A. R., Ojima, D. S., Li, C., Parton, W. J., Potter, C. S., Priesack, E., Stenger, R., Haberbosch, C., Dorsch, P., Flessa, H., and Smith, K. A., 1998. Comparison of N_2O emissions from soils at three temperate agricultural sites: simulations of year-round measurements by four models. Nutr. Cycl. Agroecosys. 52, 77–105.

Gabrielle, B. and Gagnaire, N., 2008. Life-cycle assessment of straw use in bio-ethanol production: A case study based on biophysical modelling. Biomass Bioenerg. 32, 431–441.

Gabrielle, B., Laville, P., Duval, O., Nicoullaud, B., Germon, J. C., and Hénault, C., 2006. Process-based modeling of nitrous oxide emissions from wheat-cropped soils at the subregional scale. Global Biogeochem. Cy. 20.

Gabrielle, B., Mary, B., Roche, R., Smith, P., and Gosse, G., 2002. Simulation of carbon and nitrogen dynamics in arable soils: a comparison of approaches. Eur. J. Agron. 18, 107–120.

Gabrielle, B., Menasseri, S., and Houot, S., 1995. Analysis and field-evaluation of the CERES models water-balance component. Soil Sci. Soc. Am. J. 59, 1403–1412.

Galloway, J. N., Townsend, A. R., Erisman, J. W., Bekunda, M., Cai, Z. C., Freney, J. R., Martinelli, L. A., Seitzinger, S. P., and Sutton, M. A., 2008. Transformation of the nitrogen cycle: Recent trends, questions, and potential solutions. Science 320, 889–892.

Gelman, A. and Rubin, D. B., 1992. Inference from iterative simulation using multiple sequences. Stat. Sci. 7, 457–472.

Gijsman, A. J., Hoogenboom, G., Parton, W. J., and Kerridge, P. C., 2002. Modifying DSSAT crop models for low-input agricultural systems using a soil organic matter-residue module from CENTURY. Agron. J. 94, 462–474.

Gosse, G., Cellier, P., Denoroy, P., Gabrielle, B., Laville, P., Leviel, B., Justes, E., Nicolardot, B., Mary, B., Recous, S., Germon, J. C., Hénault, C., and Leech, P. K., 1999. Water, carbon and nitrogen cycling in a rendzina soil cropped with winter oilseed rape: the Chalons Oilseed Rape Database. Agronomie 19, 119–124.

Grant, R. F., Arkebauer, T. J., Dobermann, A., Hubbard, K. G., Schimelfenig, T. T., Suyker, A. E., Verma, S. B., and Walters, D. T., 2007. Net Biome Productivity of Irrigated and Rainfed Maize Soybean Rotations: Modeling vs. Measurements. Agron. J. 99, 1404–1423.

Grant, R.F., Pattey, E., 1999. Mathematical modeling of nitrous oxide emissions from an agricultural field during spring thaw. Global Biogeochem. Cycles 13, 679–694.

Hénault, C., Bizouard, F., Laville, P., Gabrielle, B., Nicoullaud, B., Germon, J. C., and Cellier, P., 2005. Predicting in situ soil $N-2O$ emission using NOE algorithm and soil database. Glob. Change Biol. 11, 115–127.

Hutchinson, G. L. and Davidson, E. A., 1993. Processes for Production and Consumption of Gaseous Nitrogen Oxides in Soil. In Rolston, D., Duxbury, J., Harper, L., and Mosier, A., editors, Agricultural Ecosystem Effects on trace Gases and Global Climate Change chapter 5. ASA Special publication 55.

IPCC, 2007. Climate Change 2007 - The Physical Science Basis: Working Group I Contribution to the Fourth Assessment Report of the IPCC (Climate Change 2007). Cambridge University Press.

Jones, C. A. and Kiniry, J. R., 1986. CERES-N Maize: a simulation model of maize growth and development. Texas A&M University Press, College Statio, Temple, TX.

Jungkunst, H. F., Freibauer, A., Neufeldt, H., and Bareth, G., 2006. Nitrous oxide emissions from agricultural land use in Germany - a synthesis of available annual field data. J. Plant Nutr. Soil Sc. 169, 341–351.

Kaiser, E. A. and Ruser, R., 2000. Nitrous oxide emissions from arable soils in Germany - An evaluation of six long-term field experiments. J. Plant Nutr. Soil Sc. 163, 249–259.

Kim, S. and Dale, B. E., 2005. Environmental aspects of ethanol derived from no-tilled corn grain: nonrenewable energy consumption and greenhouse gas emissions. Biomass Bioenerg. 28, 475–489.

Lamboni, M., Makowski, D., Lehuger, S., Gabrielle, B., and Monod, H., 2009. Multivariate global sensitivity analysis for dynamic crop models. Field Crops Res. 113, 312–320.

Laville, P., Lehuger, S., Loubet, B., Chaumartin, F., and Cellier, P., 2011. Effect of management, climate and soil conditions on N_2O and NO emissions from an arable crop rotation using high temporal resolution measurements. Agr. Forest Meteorol. 151,228–240.

Lehuger, S., Gabrielle, B., Cellier, P., Loubet, B., Roche, R., Béziat, P., Ceschia, E., and M., W., 2010. Predicting the net carbon exchanges of crop rotations in Europe with an agro-ecosystem model. Agr. Ecosyst. Environ. 139, 384–395.

Lehuger, S., Gabrielle, B., van Oijen, M., Makowski, D., Germon, J.-C., Morvan, T., and Hénault, C., 2009. Bayesian calibration of the nitrous oxide emission module of an agro-ecosystem model. Agr. Ecosyst. Environ 133, 208 – 222.

Li, C. S., Frolking, S., and Butterbach-Bahl, K., 2005a. Carbon sequestration in arable soils is likely to increase nitrous oxide emissions, offsetting reductions in climate radiative forcing. Climatic Change 72, 321–338.

Li, C. S., Frolking, S., and Frolking, T. A., 1992. A Model of Nitrous-oxide Evolution From Soil Driven by Rainfall Events .1. Model Structure and Sensitivity. J. Geophys. Res-Atmos. 97, 9759–9776.

Li, Y., Chen, D. L., Zhang, Y. M., Edis, R., and Ding, H., 2005b. Comparison of three modeling approaches for simulating denitrification and nitrous oxide emissions from loam-textured arable soils. Global Biogeochem. Cy. 19.

Loubet, B., Laville, P., Lehuger, S., Larmanou, E., Fléchard, C., Mascher, N., Génermont, S., Roche, R., Ferrrara, R., Stella, P., Personne, E., Durand, B., Decuq, C., Flura, D., Masson, S., Fanucci, O., Rampon, J.-N., Siemens, J., Kindler, R., Gabrielle, B., Schrumpf, M., Cellier, P., 2011. Carbon, nitrogen and GHG budgets over a four years crop rotation in Northern France. Plant and Soil (in press).

Metropolis, N., Rosenbluth, A. W., Rosenbluth, M. N., Teller, A. H., and Teller, E., 1953. Equation of state calculations by fast computing machines. J. Chem. Phys. 21, 1087–1092.

Mosier, A. R., Halvorson, A. D., Peterson, G. A., Robertson, G. P., and Sherrod, L., 2005. Measurement of net global warming potential in three agroecosystems. Nutr. Cycl. Agroecosys. 72, 67–76.

Neftel, A. and Flechard, C. and Ammann, C. and Conen, F. and Emmenegger, L. and Zeyer, K. Experimental assessment of N_2O background fluxes in grassland systems. Tellus B 59, 470–482.

Nemecek, T., Heil, A., Huguenin, O., Erzinger, S., Blaser, S., Dux, D., and Zimmerman, A., 2003. Life Cycle Inventories of Production Systems. Final report Ecoinvent 2000, No 15. FAL Reckenholz, FAT Tanikon, Swiss Centre For Life Cycle Inventories, Dubendorf, CH.

Pathak, H., Li, C., and Wassmann, R., 2005. Greenhouse gas emissions from Indian rice fields: calibration and upscaling using the DNDC model. Biogeosciences 2, 113–123.

Robertson, G. P. and Grace, P. R., 2004. Greenhouse gas fluxes in tropical and temperate agriculture: The need for a full-cost accounting of global warming potentials. Environ., Dev. and Sustain. 6, 51–63.

Robertson, G. P., Paul, E. A., and Harwood, R. R., 2000. Greenhouse gases in intensive agriculture: Contributions of individual gases to the radiative forcing of the atmosphere. Science 289, 1922–1925.

Rolland, M.-N., Gabrielle, B., Laville, P., Cellier, P., Beekmann, M., Gilliot, J.-M., Michelin, J., Hadjar, D., and Curci, G., 2010. High-resolution inventory of NO emissions from agricultural soils over the Ile-de-France region. Environ. Pollut. 158, 711–722.

Six, J., Ogle, S. M., Breidt, F. J., Conant, R. T., Mosier, A. R., and Paustian, K., 2004. The potential to mitigate global warming with no-tillage management is only realized when practised in the long term. Glob. Change Biol. 10, 155–160.

Skiba, U., Drewer, J., Tang, Y., van Dijk, N., Helfter, C., Nemitz, E., Famulari, D., Cape, J., Jones, S., Twigg, M., Pihlatie, M., Vesala, T., Larsen, K., Carter, M., Ambus, P., Ibrom, A., Beier, C., Hensen, A., Frumau, A., Erisman, J., Brüggemann, N., Gasche, R., Butterbach-Bahl, K., Neftel, A., Spirig, C., Horvath, L., Freibauer, A., Cellier, P., Laville, P., Loubet, B., Magliulo, E., Bertolini, T., Seufert, G., Andersson, M., Manca, G., Laurila, T., Aurela, M., Lohila, A., Zechmeister-Boltenstern, S., Kitzler, B., Schaufler, G., Siemens, J., Kindler, R., Flechard, C., Sutton, M., 2009. Biosphere-atmosphere exchange of reactive nitrogen and greenhouse gases at the NitroEurope core flux measurement sites: Measurement strategy and first data sets. Agr. Ecosyst. Environ 133, 139–149.

Smith, P., Goulding, K. W., Smith, K. A., Powlson, D. S., Smith, J. U., Falloon, P., and Coleman, K., 2001. Enhancing the carbon sink in European agricultural soils: including trace gas fluxes in estimates of carbon mitigation potential. Nutr. Cycl. Agroecosys. 60, 237–252.

Smith, P., Martino, D., Cai, Z., Gwary, D., Janzen, H., Kumar, P., McCarl, B., Ogle, S., O'Mara, F., Rice, C., Scholes, B., and Sirotenko, O., 2007. Agriculture. In Climate Change 2007: Mitigation. Contribution of Working Group III to the Fourth Assessment Report of the Intergovernmental Panel on Climate Change, [B. Metz, O.R. Davidson, P.R. Bosch, R. Dave, L.A. Meyer (eds)]. Cambridge University Press, Cambridge, United Kingdom and New York, NY, USA.

Sutton, M. A., Nemitz, E., Erisman, J. W., Beier, C., Bahl, K. B., Cellier, P., de Vries, W., Cotrufo, F., Skiba, U., C., D. M., Jones, S., Laville, P., Soussana, J. F., Loubet, B., Twigg, M., Famulari, D., Whitehead, J., Gallagher, M. W., Neftel, A., Flechard, C. R., Herrmann, B., Calanca, P. L., Schjoerring, J. K., Daemmgen, U., Horvath, L., Tang, Y. S., Emmett, B. A., Tietema, A., Penuelas, J., Kesik, M., Brueggemann, N., Pilegaard, K., Vesala, T., Campbell, C. L., Olesen, J. E., Dragosits, U., Theobald, M. R., Levy, P., Mobbs, D. C.,

Milne, R., Viovy, N., Vuichard, N., Smith, J. U., Smith, P., Bergamaschi, P., Fowler, D., and Reis, S., 2007. Challenges in quantifying biosphere-atmosphere exchange of nitrogen species. Environ. Pollut. 150, 125–139.

Tilman, D., 1999. Global environmental impacts of agricultural expansion: The need for sustainable and efficient practices. Proc. Natl. Acad. Sci. 96, 5995–6000.

Trinsoutrot, I., Nicolardot, B., Justes, E., and Recous, S., 2000. Decomposition in the field of residues of oilseed rape grown at two levels of nitrogen fertilisation. Effects on the dynamics of soil mineral nitrogen between successive crops. Nutr. Cycl. Agroecosys. 56, 125–137.

Van Oijen, M., Rougier, J., and Smith, R., 2005. Bayesian calibration of process-based forest models: bridging the gap between models and data. Tree Physiol. 25, 915–927.

Wallach, D., 2006. Evaluating crop models. In Wallach, D., Makowski, D., and Jones, J. W., editors, Working with dynamic crop models: evaluating, analyzing, parameterizing and using them chapter 2. Elsevier.

West, T. O. and Marland, G., 2002. Net carbon flux from agricultural ecosystems: methodology for full carbon cycle analyses. Environ. Pollut. 116, 439–444.

Zhang, Y., Li, C., Zhou, X., and Moore, B., 2002. A simulation model linking crop growth and soil biogeochemistry for sustainable agriculture. Ecol. Model. 151, 75–108.

List of Tables

Table 1: Experimental treatments, N input rates and monitoring periods for the GHGs at the Grignon, Rafidin and Gebesee sites.

Site	Crop	Sowing date	N Fertilizer		Monitoring period		
			Date	Amount (kg N ha^{-1})	CO_2	N_2O	CH_4
RAFIDIN	Rapeseed N0	04/09/1994					
	Rapeseed N1	04/09/1994	20/02/1995	80			
			15/03/1995	75			
	Rapeseed N2	04/09/1994	12/09/1994	49			
			20/02/1995	80			
			15/03/1995	75			
			29/03/1995	38			
	Wheat	27/10/1995	10/02/1996	60			
			10/03/1996	95			
			10/05/1996	65			
	Barley	27/10/1995	10/02/1997	90			
			10/03/1997	80			
GRIGNON-PP	Wheat	16/10/2002	26/02/2003	52			
			27/03/2003	60			
	Barley	17/10/2003	18/02/2004	59			
			19/03/2004	59			
			02/04/2004	39			
	Mustard	02/09/2004	31/08/2004	Slurry (60)			
	Maize	09/05/2005	09/05/2005	140			
	Wheat	16/10/2005	15/03/2006	55			
			14/04/2006	55			
	Barley	06/10/2006	22/02/2007	55			
			22/03/2007	55			
	Mustard	22/09/2007	17/04/2008	Slurry (80)			
	Maize	28/04/2008	05/05/2008	60			
GRIGNON-PAN1	Wheat	27/10/2005	06/03/2006	50			
			07/04/2006	110			
	Barley	06/10/2006	04/03/2007	50			
			26/03/2007	70			
	Mustard	31/08/2007					
	Maize	07/05/2008	08/05/2008	140			
GRIGNON-PAN2	Barley	05/10/2005	06/03/2006	50			
			07/04/2006	50			
	Mustard	30/09/2006					
	Maize	26/04/2007	02/05/2007	150			
	Wheat	24/10/2007	14/02/2008	50			
			03/04/2008	120			
			15/05/2008	40			
GRIGNON-PAN3	Mustard	02/09/2005					
	Maize	26/04/2006	04/05/2006	160			
	Wheat	10/10/2006	05/03/2007	50			
			26/03/2007	70			
	Barley	08/10/2007	15/02/2008	50			
			05/04/2008	90			
GEBESEE	Sugar beet	20/10/2006	10/04/2006	30			
	Wheat	27/10/2006	27/03/2007	80			
			11/04/2007	Slurry (20)			
			03/05/2007	85			
			03/09/2007	FYM (200)			

14/09/1994 - 14/04/1995

18/05/2004 - 30/10/2008 | 01/01/2007 - 31/08/2008 | 11/07/2007 - 04/09/2008

11/07/2007 - 04/09/2008 | 11/07/2007 - 04/09/2008

01/01/2007- 06/11/2007 | 27/02/2006- 27/12/2007

Table 2: Greenhouse gases emitted by the production and transportation of fertilizers and pesticides, the cropping operations and the input transportation at the farm. Greenhouse gas emission factors are expressed with reference to different units (kg, ha, t km). The contribution of CO_2, CH_4 and N_2O to the emissions were computed for each step. Data for indirect emissions are all from the Ecoinvent database (Nemecek et al., 2003).

Source of indirect emissions	Life cycles	Products and machinery	Reference unit	GHG emissions	CO_2	CH_4	N_2O
				kg CO_2-C eq	Contribution in %		
Agricultural inputs	Production and transport at the regional storehouse	Ammonium nitrate	kg N	2.28	32	0.9	67
	Production and transport at the regional storehouse	Urea	kg N	1.5	47	1.5	51
	Production and transport at the regional storehouse	Pesticide	kg active ingredient	1.95	95.7	3.4	0.8
Cropping operations	Ploughing	Plough	ha	31.1	96.2	2.7	0.9
	Cultivating	Chisel	ha	18.6	96.2	2.7	0.9
	Harrowing	Rotary harrow	ha	15.7	96.0	2.8	0.9
	Harrowing	Spring tine harrow	ha	6.2	96.0	3.0	0.9
	Sowing	Seeder	ha	5.7	96.0	2.9	0.9
	Fertilizer application	Broadcaster	ha	6.6	96.1	2.8	0.9
	Slurry spreading	Slurry tanker	m3	0.3	95.9	3.1	0.9
	Application of plant protection products	Field sprayer	ha	2.7	95.8	3.2	0.9
	Harvesting	Combine harvesting	ha	40.4	96.1	2.8	0.9
Input transportation at the farm	Fertilizer transportation	Barge	t km	0.17	96.2	1.5	2.2
	Fertilizer transport	Freight, rail	t km	0.01	96.0	2.9	0.9
	Fertilizer transport	Lorry	t km	0.04	96.8	1.8	0.9
	Pesticide transport	Van	t km	0.3	96.5	2.0	1.4

Table 3: Description of the 6 parameters selected for the calibration of the N_2O emissions module. The prior probability distribution is defined as multivariate uniform between bounds θ_{min} and θ_{max}. The posterior parameter distributions are based on the calibration with the Grignon-PP data set, and are characterized by the mean value of the posterior, their standard deviation (SD). Correlations with other parameters are reported if their absolute value exceeds 0.4 (underlined parameters express a negative correlation).

Parameter vector $\theta = [\theta_1 ... \theta_6]$					Prior probability distribution		Posterior probability distribution		
θ_i	Symbol	Description	Unit	Default value	θ_{min}(i)	θ_{max}(i)	Mean	SD	Correlated $\{\theta_i\}$
θ_1	r	Ratio of N_2O emissions to total denitrification rate	%	0.20	0.09	0.90	0.36	0.09	{2,4,5,6}
θ_2	PDR	Potential denitrification rate	kg N ha^{-1} d^{-1}	6.0	0.1	20.0	0.33	0.61	{2,1,5,6}
θ_3	Tr_{WFPS}	WFPS threshold below which no denitrification occurs	%	0.62	0.40	0.80	0.61	0.05	{2,4,5}
θ_4	POW_{denit}	Exponent of the power law for the denitrification response function to WFPS	Unitless	1.74	0.00	2.00	0.46	0.21	{1, 3}
θ_5	Km_{denit}	Half-saturation constant of denitrification response factor to NO_3^-	mg N kg^{-1} soil	22.00	5.00	120.00	24.69	17.53	{1,2,3,6}
θ_6	TTr_{denit}	Temperature threshold between the two sequential Q10 functions of the denitrification response factor to soil temperature	°C	11.00	10.00	15.00	10.05	0.17	{1,2,5}

Table 4: Sample size (N), mean of measured in situ soil variables (Mean), mean deviation (MD) and root mean square errors (RMSE) of the following model-predicted variables: soil temperature, soil water content and topsoil nitrate and ammonium contents, for the 8 data sets.

Site	Treatment	Soil temperature				Soil water content				Nitrate content				Ammonium content			
		N	Mean	MD	RMSE	N	Mean	MD	RMSE	N	Mean	MD	RMSE	N	Mean	MD	RMSE
			(°C)				(v/v)				(kg NO_3-N ha^{-1})				(kg NH_4-N ha^{-1})		
GRIGNON	PP	637	10.9	-1.1	3.0	492	0.318	0.016	0.033	24	49.4	23.2	40.7	24	10.6	7.2	11.0
	PAN1	-	-	-	-	14	0.238	-0.039	0.064	13	36.7	-2.3	21.6	13	10.1	6.8	12.5
	PAN2	-	-	-	-	17	0.238	-0.045	0.064	16	71.9	31.2	57.0	16	17.8	14.2	23.5
	PAN3	-	-	-	-	15	0.255	-0.029	0.042	14	26.5	-3.8	22.7	14	6.1	3.4	4.9
GEBESEE		729	10.7	-0.2	3.3	649	0.260	-0.065	0.080	78	18.1	-1.1	24.5	78	7.7	4.4	28.6
RAFIDIN	N0	294	8.7	-1.2	3.0	20	0.253	-0.027	0.043	21	10.8	5.5	9.9	21	3.7	3.5	4.1
	N1	294	8.7	-1.2	3.0	20	0.244	-0.035	0.051	21	12.9	8.0	11.8	21	5.6	5.0	6.8
	N2	294	8.7	-1.2	3.0	20	0.240	-0.039	0.050	21	23.5	17.0	22.6	21	6.2	5.6	8.0

Table 5: Root mean square errors (RMSEs) of daily nitrous oxide emissions (g N-N_2O ha^{-1} d^{-1}), using either the default or calibrated set of parameters in the model. The calibrated parameter set is the posterior expectancy of parameters computed in the Bayesian calibration against the Rafidin and Grignon-PP data sets. For the Grignon-PAN1, -PAN2, -PAN3 and the Gebesee sites, the RMSEP was computed with the posterior expectancy of parameters based on the Bayesian calibration against the N_2O measurements of the Grignon-PP site.

Site	Treatment	RMSE or RMSEP (in italics) computed with:	
		Initial parameter values	Posterior expectancy of parameters
Grignon-PP		20.2	14.2
Rafidin	N0	4.6	0.3
	N1	10.4	1.4
	N2	15.9	3.0
Grignon-PAN1		10.4	*9.6*
Grignon-PAN2		7.4	*7.0*
Grignon-PAN3		7.6	*7.3*
Gebesee		7.6	*4.6*

Table 6: Predictions of net GHG balance based on simulations of net biome production (the convention sign was inversed to compute GHG balance) and N_2O emissions, estimation of methane fluxes from chamber measurements and indirect GHG of agricultural inputs. The 3-yr crop rotations were successively simulated over 36 and 28 years for Grignon-PP and Rafidin cropping systems respectively. Simulations were averaged for each crop from the first year (n) to the last year (n+2) of the rotations. The values of the complete 3-yr rotations (*Rotation*) were the total of the 4 successive crops. Numbers in bracket indicate standard deviations over the time periods.

	Time period		CO_2			N_2O	CH_4	Agricultural inputs	Net GHG balance
			NEP	Exports	NBP				
	Start	End	kg CO_2-C eq ha^{-1}						
GRIGNON-PP									
Maize	9 May n	15 Oct. n	-5828(890)	5855(864)	27(327)	179(45)	-2	310	514(348)
Wheat	16 Oct. n	5 Oct. n+1	-5301(750)	6269(682)	969(209)	235(66)	-5	324	1522(251)
Barley	6 Oct. n+1	21 Oct. n+2	-4774(634)	5129(576)	356(194)	400 (94)	-5	338	1087(212)
Mustard	22 Oct. n+2	8 May n+3	441(68)	0	-1322(68)	136(41)	3	70	-1112(55)
Rotation	9 May n	8 May n+3	-15462(1046)	17253(968)	29(381)	949(129)	-9	1042	2011(323)
RAFIDIN									
Rapeseed N0	10 Sept. n	26 Oct. n+1	-1303(1420)	1490(726)	187(867)	101(18)	-	99	387(857)
Wheat	27 Oct n+1	26 Oct n+2	-5194(1253)	3493(1163)	-1701(595)	128(41)	-	471	-1102(626)
Barley	27 Oct n+2	9 Sept. n+3	-3149(698)	3088(489)	-61(378)	108(43)	-	397	444(388)
Rotation N0	10 Sept. n	9 Sept. n+3	-9646(1772)	8071(1742)	-1575(606)	338(71)	-	967	-270(603)
Rapeseed N1	10 Sept. n	26 Oct. n+1	-4263(995)	2413(260)	-1850(1003)	121(27)	-	359	-1370(1010)
Wheat	27 Oct n+1	26 Oct n+2	-4877(1111)	3521(1127)	-1355(462)	135(44)	-	471	-750(484)
Barley	27 Oct n+2	9 Sept. n+3	-3376(707)	3121(501)	-255(493)	117(44)	-	397	258(486)
Rotation N1	10 Sept. n	9 Sept. n+3	-12516(1691)	9056(1417)	-3460(1110)	372(78)	-	1226	-1862(1133)
Rapeseed N2	10 Sept. n	26 Oct. n+1	-4639(1168)	2481(247)	-2158(1158)	159(28)	-	506	-1493(1169)
Wheat	27 Oct n+1	26 Oct n+2	-4889(1101)	3350(1131)	-1339(453)	136(45)	-	471	-732(471)
Barley	27 Oct n+2	9 Sept. n+3	-3440(716)	3130(505)	-309(536)	119(44)	-	397	206(530)
Rotation N2	10 Sept. n	9 Sept. n+3	-12968(1836)	9162(1439)	-3806(1211)	414(116)	-	1374	-2019(1232)

Table 7: Predictions of net GHG balance based on simulations of net biome production (the convention sign was inversed to compute GHG balance) and N_2O emissions, estimation of methane fluxes from chamber measurements and indirect GHG costs of agricultural inputs, for the one-year wheat crop cycle of Gebesee and the three treatments PAN1, PAN2 and PAN3 of Grignon. These last 3 treatments were simulated with the same soil and climate parameters and the same rotation but with 0, 1 and 2 years time lag interval in the crop sequence in order to have all the crops each year. The values of the complete rotations (*Rotation*) were the total of the 4 successive crops.

	Time period		CO_2			N_2O	CH_4	Agricultural inputs	Net GHG balance
			NEP	Exports	NBP				
	Start	End	kg CO_2-C eq ha^{-1}						
GRIGNON-PAN1									
Wheat	27/10/05	05/10/06	-3907	5494	1587	117	-6	371	2070
Barley	06/10/06	30/08/07	-5368	5159	-209	208	-5	475	469
Mustard	31/08/07	06/05/08	579	0	579	101	-4	109	784
Maize	07/05/08	26/10/08	-4127	1916	-2211	119	-3	299	-1796
Rotation	27/10/05	26/10/08	-12823	12569	-254	545	-18	1253	1526
GRIGNON-PAN2									
Barley	05/10/05	29/09/06	-3929	4477	548	154	-13	224	913
Mustard	30/09/06	25/04/07	537	0	537	164	-8	115	808
Maize	26/04/07	23/10/07	-6984	4675	-2310	140	-7	448	-1729
Wheat	24/10/07	04/10/08	-3863	5857	1994	123	-13	643	2747
Rotation	05/10/05	04/10/08	-14240	15009	769	580	-40	1430	2739
GRIGNON-PAN3									
Mustard	02/09/05	25/04/06	372	0	372	71	-3	45	485
Maize	26/04/06	09/10/06	-5222	2630	-2592	80	-2	241	-2274
Wheat	10/10/06	07/10/07	-4895	6917	2023	221	-4	455	2695
Barley	08/10/07	01/09/08	-4687	4788	101	139	-4	497	734
Rotation	02/09/05	01/09/08	-14431	14335	-97	511	-12	1238	1640
GEBESEE									
Wheat	27/10/06	05/10/07	-2378	3066	-3773	158	-4	589	-3030

List of Figures

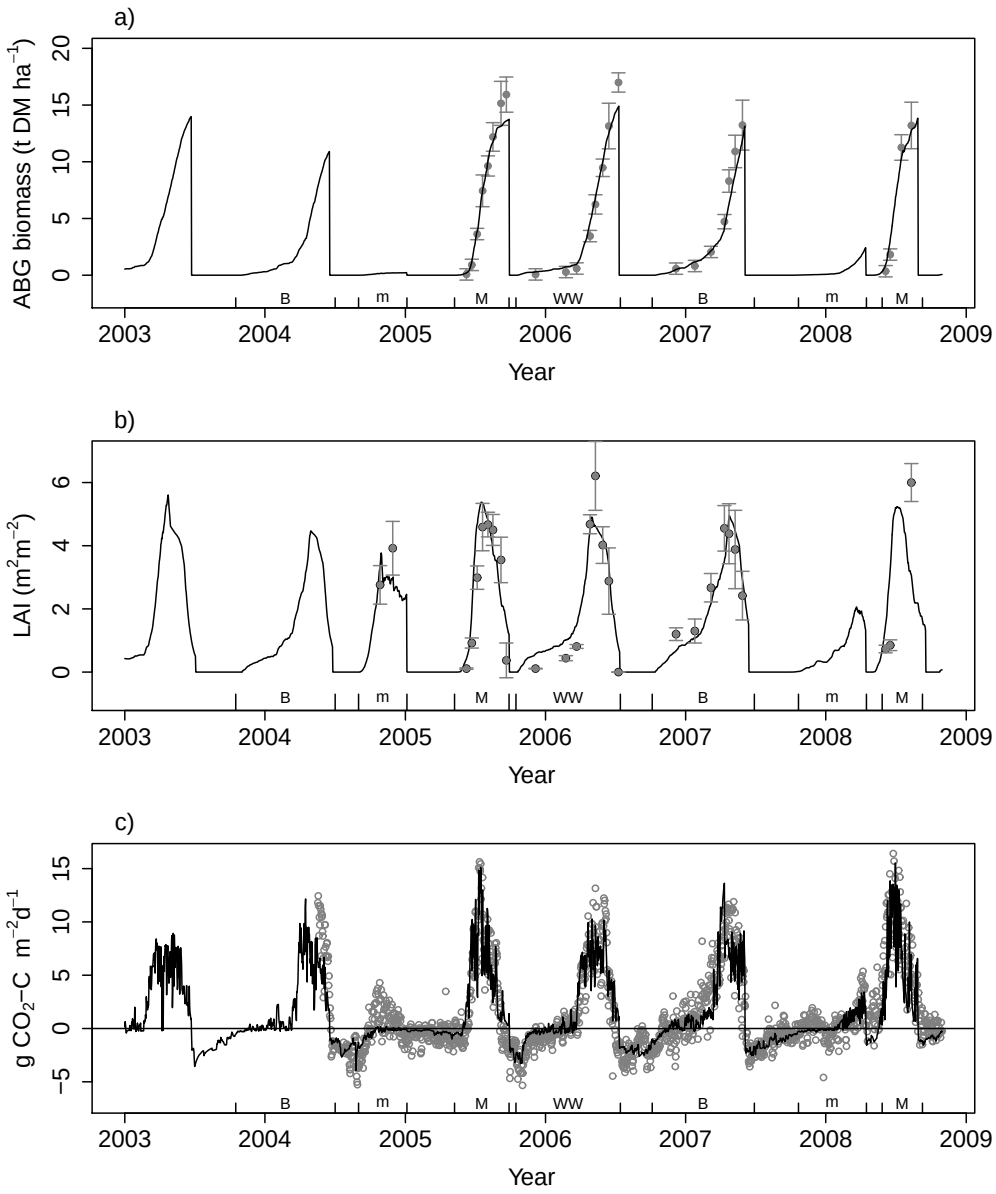

Figure 1: Simulations (black line) and observations (grey points ± sd) of above-ground (ABG) crop biomass (a), leaf area index (b) and net ecosystem production (NEP) on a daily time scale (b), at the Grignon-PP experimental field (M : maize ; WW : wheat ; B : barley ; m : mustard).

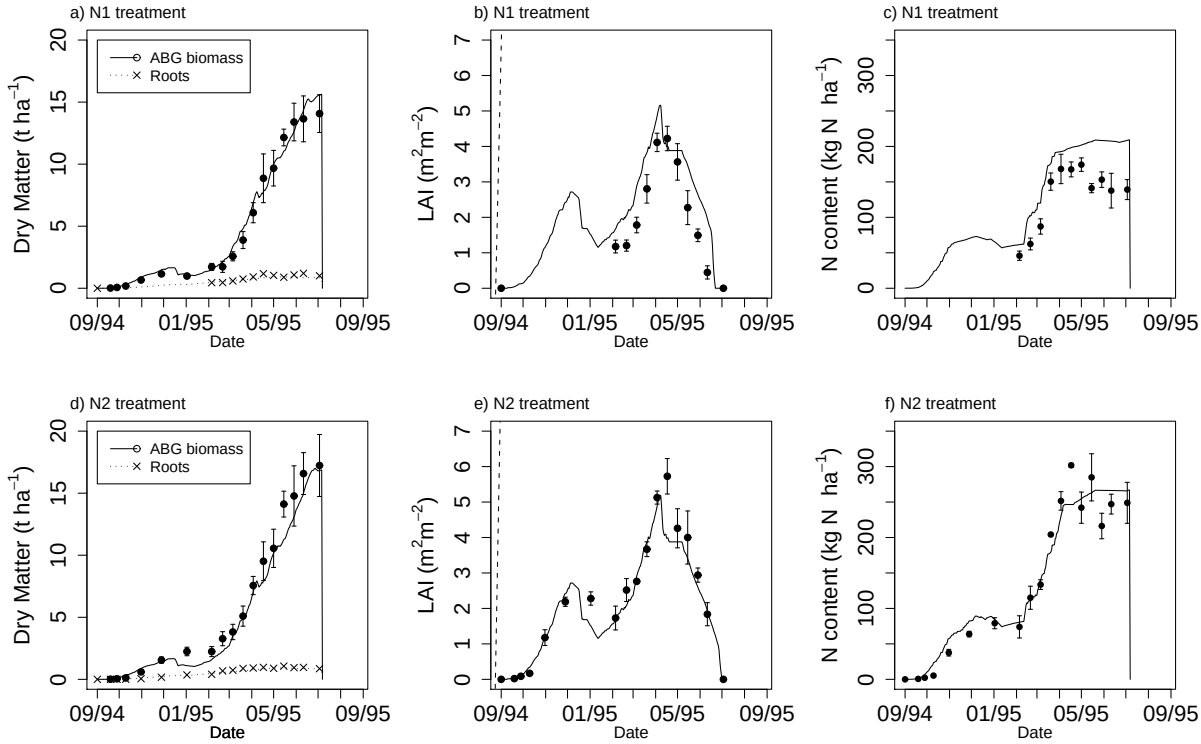

Figure 2: Simulated (lines) and measured (symbols $\pm$ sd) data for above ground (ABG) dry matter and roots of rapeseed (a, d) , leaf area index (b, e), N plant content (c, f) for N1 and N2 treatments,respectively, in 1994-1995 at Rafidin (France).

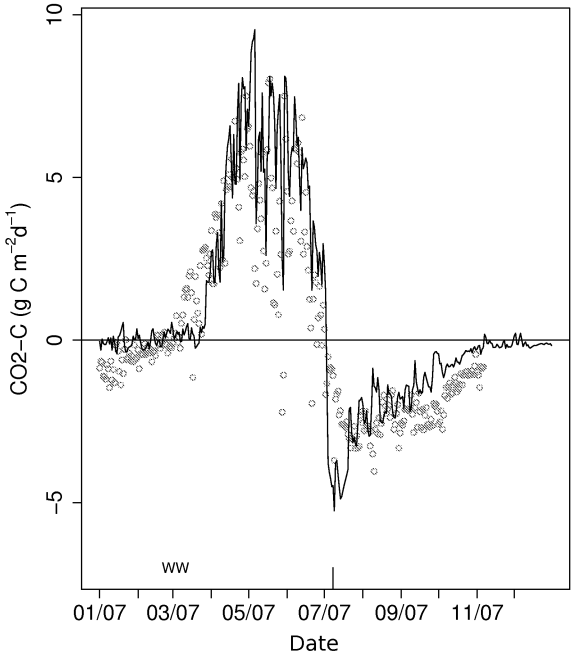

Figure 3: Simulated (black line) and observed (grey points) daily net ecosystem production (NEP) for the wheat crop cycle at Gebesee from Jan. to Oct. 2007.

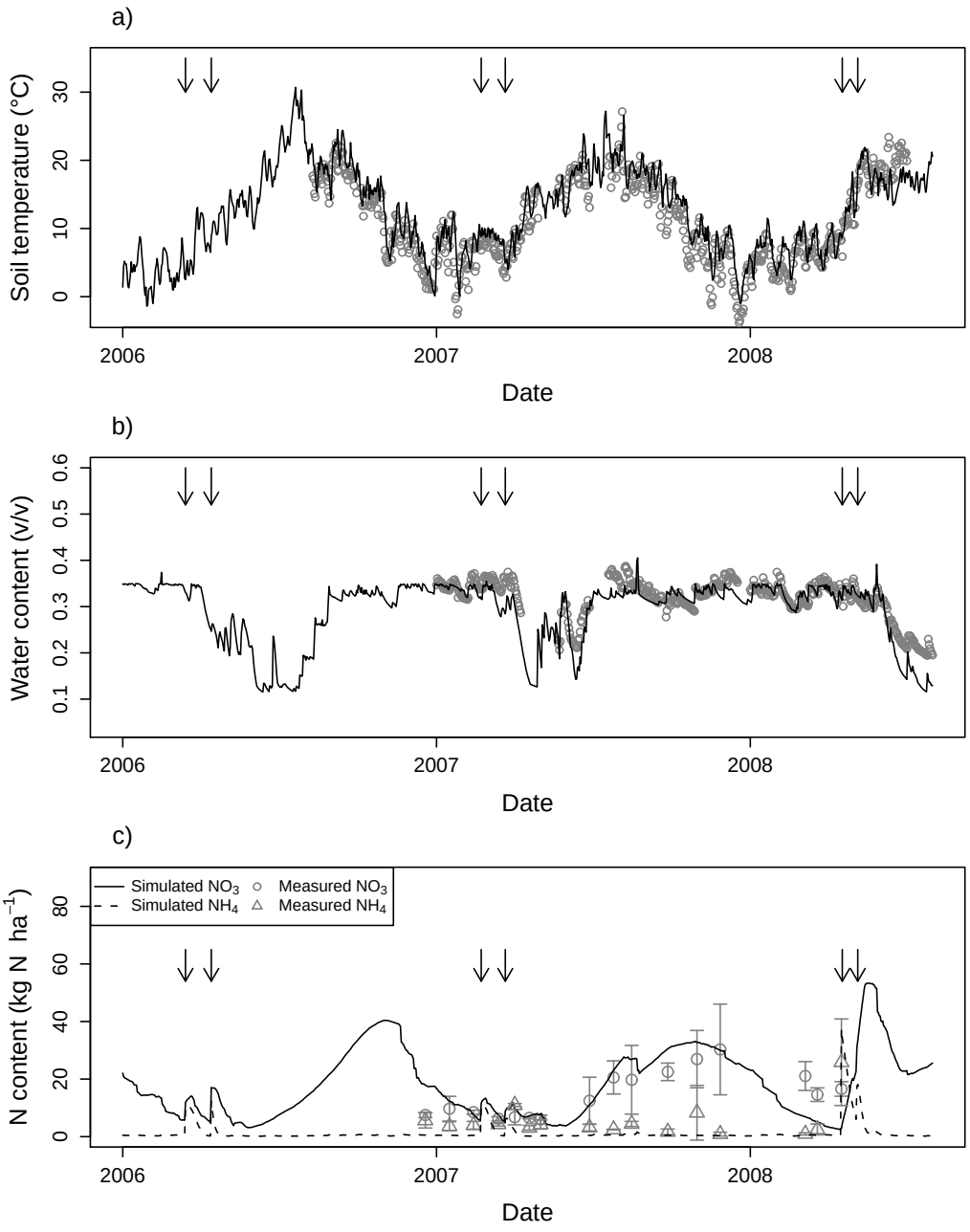

Figure 4: Simulated (line) and observed (symbols $\pm sd$) daily soil temperature (a), soil water content (b) and nitrogen content in the 0-15 cm topsoil layer (c), for the experimental field site of Grignon-PP. Arrows show time of the fertilizer applications.

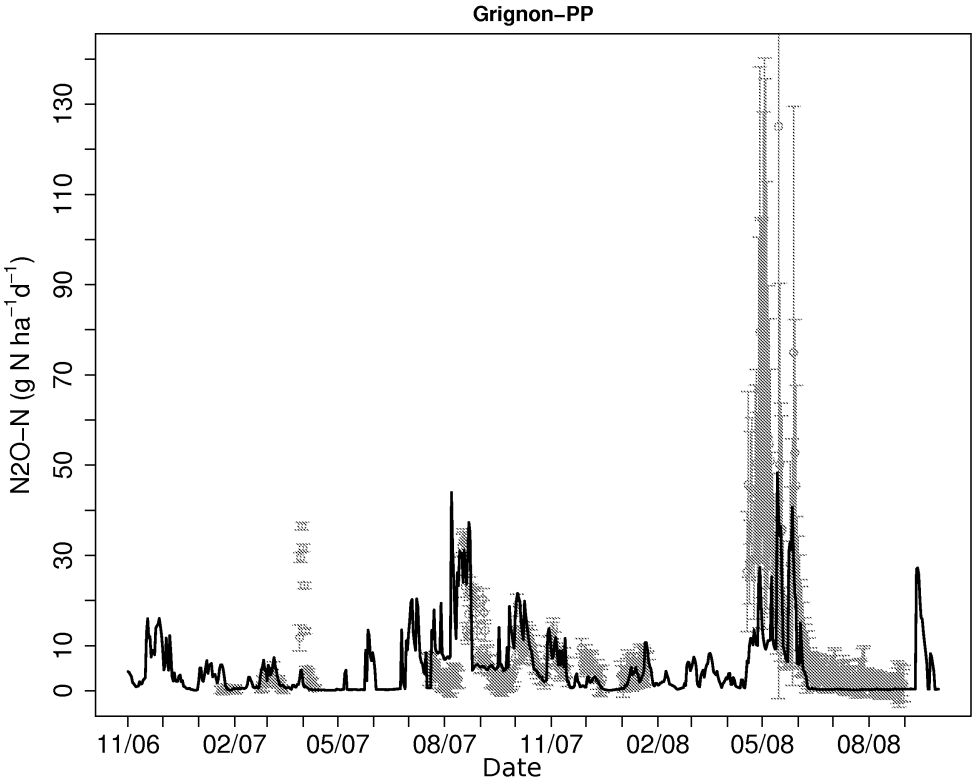

Figure 5: Simulated (black line) and observed (symbols $\pm sd$) daily nitrous oxide emissions for the Grignon-PP experimental site.

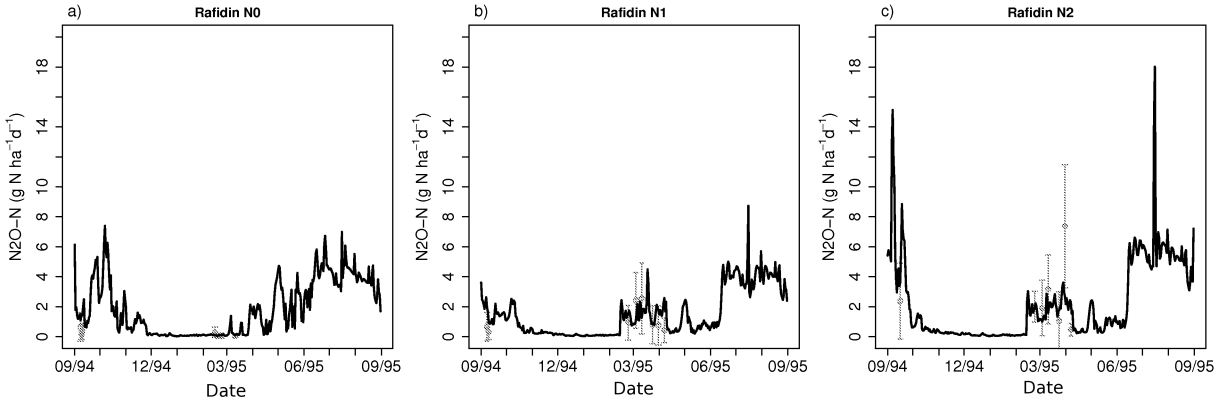

Figure 6: Simulated (line) and observed (symbols $\pm sd$) daily nitrous oxide emissions for the N0 (a), N1 (b) and N2 treatment (c) of the Rafidin experimental site.

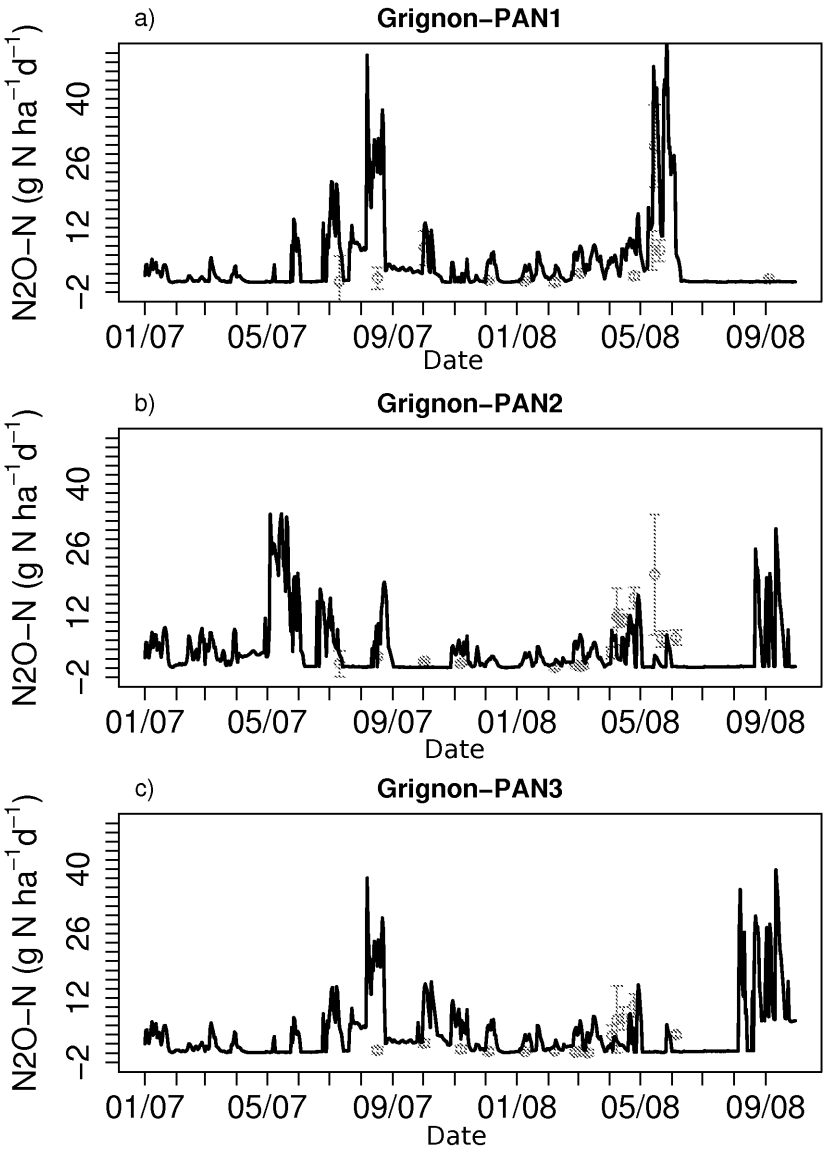

Figure 7: Simulated (line) and observed (symbols $\pm sd$) daily nitrous oxide emissions for the Grignon-PAN1 (a), -PAN2 (b) and -PAN3 (c) experiments.

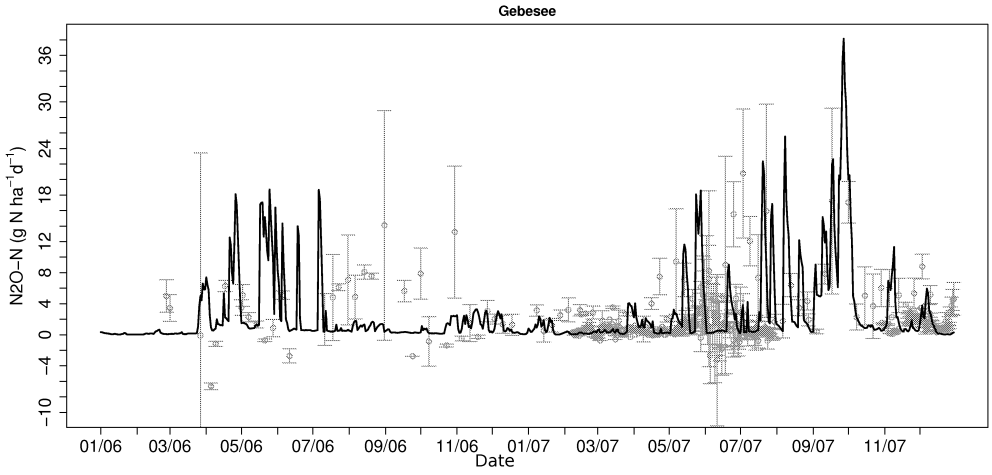

Figure 8: Simulated (line) and observed (symbols $\pm sd$) daily nitrous oxide emissions for the Gebesee experimental field site.

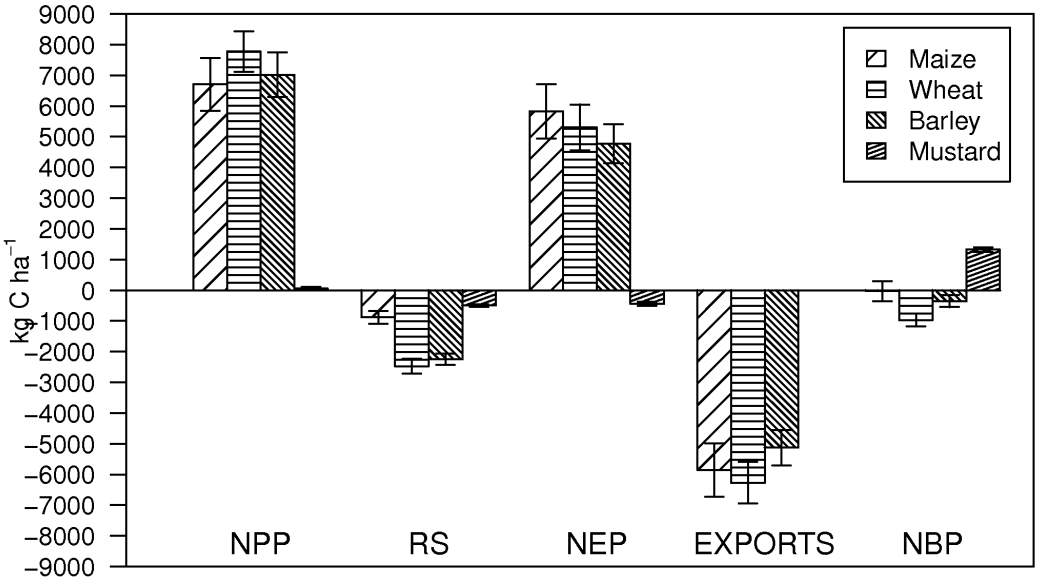

Figure 9: Breakdown of net biome production (NBP) estimated by the model into net primary production (NPP), soil respiration (Rs), net ecosystem production (NEP), grain or silage exports plus straw removal (EXPORTS) for the four crops of the rotation (maize, wheat, barley, mustard) estimated over the 36-yr simulation period at the Grignon-PP experimental site. Error bars indicate standard deviations over the time period.

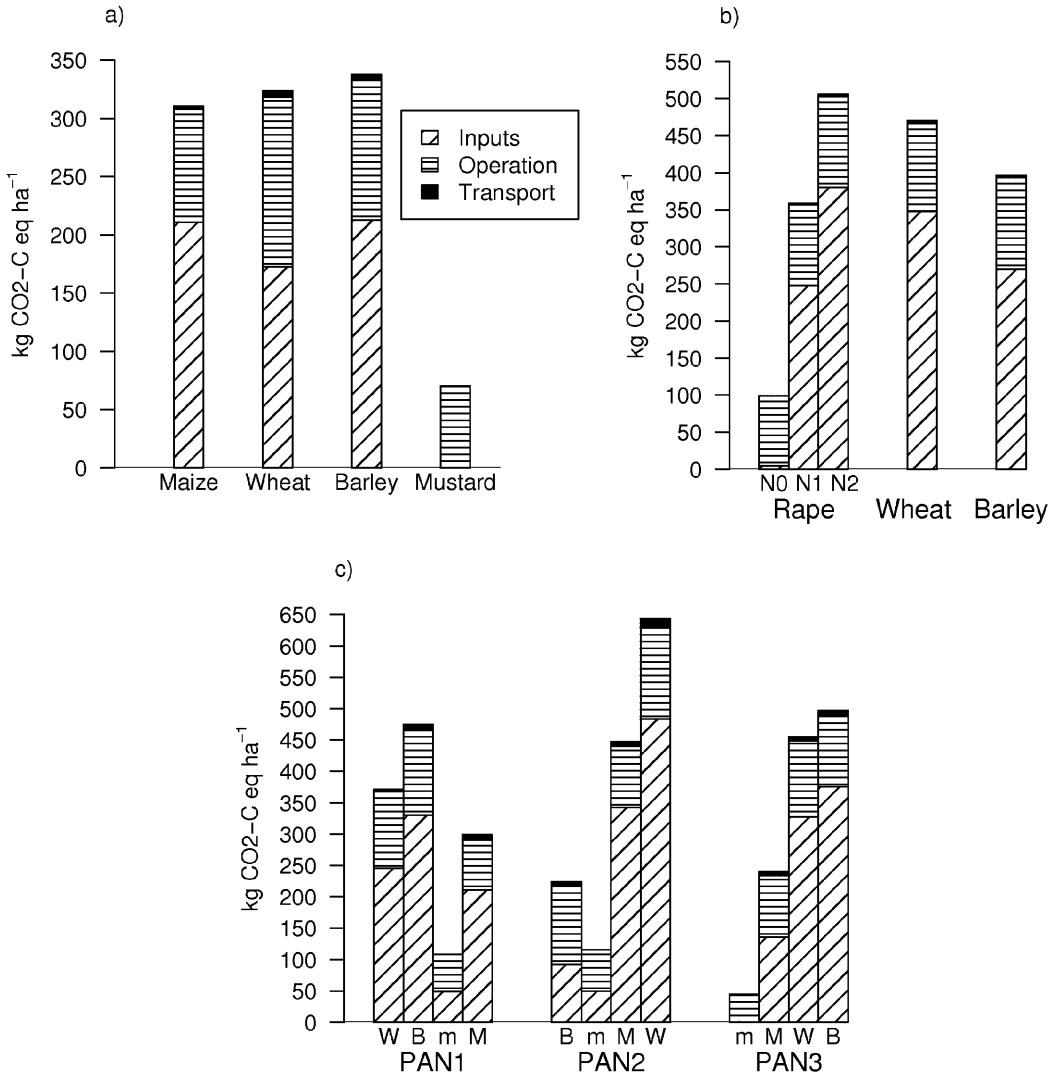

Figure 10: Greenhouse gas of agricultural inputs and cropping operations for crop production (indirect emissions) for the Grignon-PP (a), Rafidin (b) and Grignon-PANs (c) cropping systems. The emissions are broken down into the input production, agricultural operations and transport steps. Mustard was grown as catch crop which was not harvested and transported and did not receive any agricultural input. In sub-figure c, maize, wheat, barley and mustard are designated by M, W, B and m).

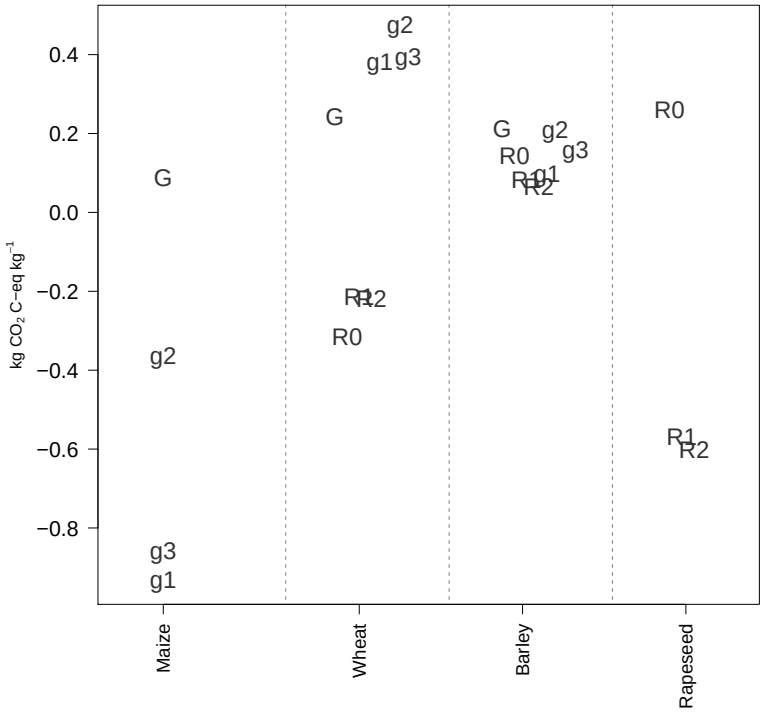

Figure 11: Comparison of the crop GHG intensities (ratio of the net GHG balance over the exported C) for the Grignon-PP (G), Grignon-PANs (PAN1=g1, PAN2=g2, PAN3=g3) and Rafidin treatments (N0=R0, N1=R1, N2=R2). The points for Grignon-PP and Rafidin treatments are the mean values over the rotation sequences and the values of Grignon-PANs are the unique values from the simulation period 2005-2008.

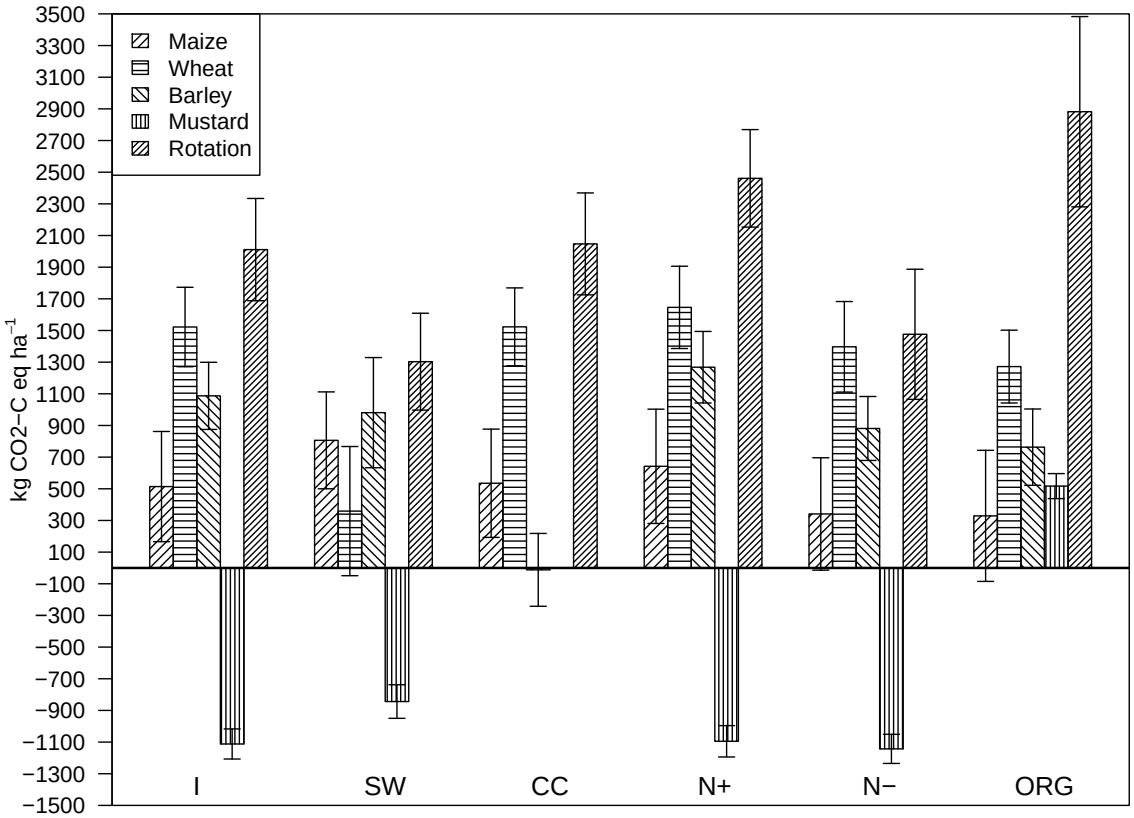

Figure 12: Comparison of net GHG balances of five scenarios averaged over 36-years for the Grignon-PP experiment. Error bars indicate standard deviations over the time periods. I: initial scenario, SW: straw left on soil, CC: without catch crop, N+: 50% more N fertilizer, N-: 50% less N fertilizer, ORG: without organic fertilizer.